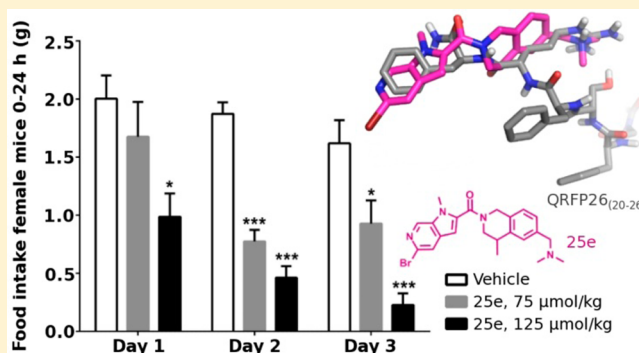


GPR103 Antagonists Demonstrating Anorexigenic Activity in Vivo: Design and Development of Pyrrolo[2,3-*c*]pyridines That Mimic the C-Terminal Arg-Phe Motif of QRFP26Jennie Georgsson,[†] Fredrik Bergström,[‡] Anneli Nordqvist,^{*,†} Martin J. Watson,[§] Charles D. Blundell,[§] Magnus J. Johansson,[†] Annika U. Petersson,[⊥] Zhong-Qing Yuan,[†] Yiqun Zhou,[#] Lisbeth Kristensson,⁺ Dorota Kakol-Palm,^{||} Christian Tyrchan,[⊥] Eric Wellner,[†] Udo Bauer,[†] Peter Brodin,^{||} and Anette Svensson Henriksson[†][†]CVMD Medicinal Chemistry, [‡]CVMD DMPK, ^{||}CVMD Bioscience, ⁺Discovery Sciences, and [⊥]RIA Medicinal Chemistry, AstraZeneca, Pepparedsleden 1, 431 83 Mölndal, Sweden[§]C4X Discovery Ltd., Unit 310 Ducie House, Ducie Street, Manchester M1 2JW, U.K.[#]Pharmaron Beijing, Co. Ltd., 6 Taihe Road, BDA, Beijing, 100176, P. R. China

S Supporting Information

ABSTRACT: GPR103, a G-protein coupled receptor, has been reported to have orexigenic properties through activation by the endogenous neuropeptide ligands QRFP26 and QRFP43. Recognizing that central administration of QRFP26 and QRFP43 increases high fat food intake in rats, we decided to investigate if antagonists of GPR103 could play a role in managing feeding behaviors. Here we present the development of a new series of pyrrolo[2,3-*c*]pyridines as GPR103 small molecule antagonists with GPR103 affinity, drug metabolism and pharmacokinetics and safety parameters suitable for drug development. In a preclinical obesity model measuring food intake, the anorexigenic effect of a pyrrolo[2,3-*c*]pyridine GPR103 antagonist was demonstrated. In addition, the dynamic 3D solution structure of the C-terminal heptapeptide of the endogenous agonist QRFP26_(20–26) was determined using NMR. The synthetic pyrrolo[2,3-*c*]pyridine antagonists were compared to this experimental structure, which displayed a possible overlay of pharmacophore features supportive for further design of GPR103 antagonists.



INTRODUCTION

Obesity is an increasing health concern related to cardiovascular diseases and diabetes.^{1,2} The pyroglutamylated RF amide peptide receptor 103 (GPR103),³ and its endogenous neuropeptide agonist ligands QRFP26 and QRFP43 (Figure 1) are

hQRFP43 QDEGSEATGFLPAAGEKTSGLGNLAEELNGYSRKKGGFSFRF-NH₂
hQRFP26 TSGPLGNLAEELNGYSRKKGGFSFRF-NH₂

Figure 1. Primary structure of human QRFP26 and QRFP43.

present in brain areas involved in feeding and body weight control in both rodents and man.^{4–8} For the human GPR103 gene there are 46 orthologues annotated. In all these species there is a one-to-one gene relationship with the exception of mouse and rat, where two closely related genes are present, GPR103A and GPR103B.⁹ Human GPR103 displays 85% amino acid identity with mouse GPR103A and 79% identity with GPR103B, while the rat GPR103A and GPR103B share respectively 84% and 82% amino acid identity with human GPR103.^{9,10}

The GPR103 neuropeptides QRFP26 and QRFP43 belong to the RF amide group of peptides, including NPFF, NPAF and PrPK. These peptides are characterized by the conserved C-terminal sequence motif Arg-Phe-NH₂.⁴ Structure–activity relationship (SAR) studies on QRFP26 have demonstrated that the C-terminal amino acids Phe24-Arg25-Phe26 are important for biological activity.¹¹ The conformation of this C-terminal motif could be supportive in the design of new GPR103 ligands. So far attempts to restrict the conformation of the three C-terminal amino acids Phe24-Arg25-Phe26 via α - β amino acids have proven unsuccessful, but other turn structures cannot be excluded.¹² NMR studies of QRFP26 have shown that the C-terminal residues are relatively unstructured.¹³

Preclinical data suggest that endogenous GPR103 neuropeptide agonists have an important regulatory role in energy homeostasis by promoting increases in food intake and body

Received: December 19, 2013

Published: June 17, 2014

weight.^{7,8,12,14} Clinical data show increased levels of QRFP26 in undernourished anorexia nervosa patients compared to healthy controls.¹⁵ Activation of GPR103 also affects nociception (inflammatory pain response),¹⁶ heart rate, and blood pressure in preclinical models.⁸ The orexigenic effect of GPR103 activation is at least partially mediated by neuropeptide Y (NPY) signaling, and it has been demonstrated that NPY1 and NPYS antagonists abolish the effect of QRFP26. Also, QRFP26 inhibits the elevation of pro-opiomelanocortin (POMC) and the anorectic effect of leptin.¹⁷ These data suggest that inhibition of the orexigenic effect of GPR103 activation can promote reduced body weight in overweight and obese patients by appetite regulation.

Only a few GPR103 antagonists from the public domain are available^{18–21} to validate the impact on energy homeostasis by inhibition of the orexigenic effect of GPR103 activation. In 2010, 3-aryl- or heteroaryl-substituted indole derivatives were claimed to antagonize the GPR103 receptor by Banyu Pharmaceutical Co Ltd.^{18–20} Two of the disclosed GPR103 antagonists are shown in Figure 2. A physicochemical

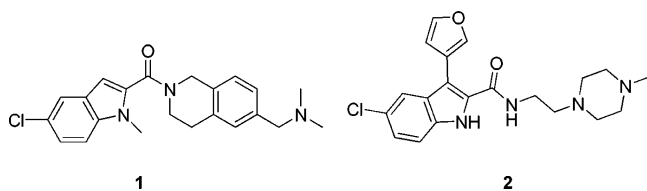


Figure 2. Two examples of disclosed GPR103 antagonists.

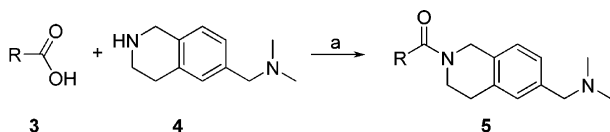
assessment of these lipophilic bases was made that displayed liabilities on metabolic stability, solubility, and CYP inhibition in addition to narrow margins to cardiac liability targets.^{22,23} Improved compound properties with retained GPR103 potency would provide high-quality leads amenable to in vivo assessment of anorexigenic efficacy.

In this paper we describe the development of a new series of GPR103 antagonists with drug metabolism and pharmacokinetics (DMPK) and safety properties suitable for drug development. From this new series, one representative compound was evaluated for modulation of appetite. An NMR study to investigate the solution conformations of the C-terminal heptapeptide QRFP26_(20–26) is also presented, with pharmacophore features of the herein developed GPR103 antagonists related to the experimental conformations of QRFP26_(20–26).

CHEMISTRY

To explore replacements for the indole motif, the tetrahydroisoquinoline (THIQ) dimethylmethylene amine was used as starting point for the synthesis of 177 diverse compounds. Outlined in Scheme 1 is the standard amide formation using

Scheme 1. Library Synthesis of THIQ Dimethylmethylene Amine Derivatives by Amide Coupling^a

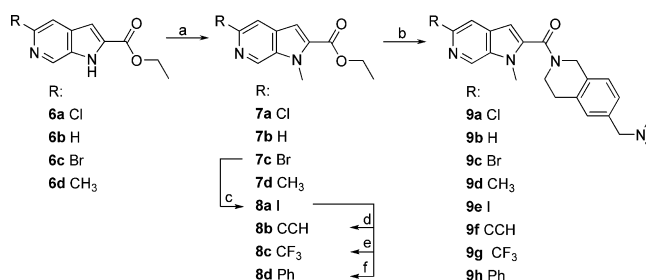


^aReagents: (a) EDC, HOBT, TEA, DMF.

EDC/HOBT as coupling reagent to generate the library with a variety of carboxylic acids (3) and the THIQ dimethylmethylene amine (4).²⁴ Among the newly identified compounds, 1-methylpyrrolo[2,3-c]pyridine-2-carboxamide with lipophilic ligand efficiency (LLE) 4.8, was taken further into optimization by investigation of the substitution pattern of the pyridine ring and substitutions on the THIQ.

Synthesis of compounds with variation in the 5-position of the pyrrolo[2,3-c]pyridine ring is outlined in Scheme 2, starting

Scheme 2. Synthesis of Compounds with Variation in the 5-Position of the Pyrrolo[2,3-c]pyridine Ring (9a–9h)^a



^aReagents: (a) CH₃I, Cs₂CO₃, DMF, rt, 16 h. (b) Method A: NaOH, EtOH:H₂O (10:1), rt followed by acid (7a, 7c, 7d, 8b and 8c) (1 equiv), 4 (1 equiv), TBTU (1.1 equiv), DIEA, DMF, rt, 18 h. Method B: ester (7b, 8d) (1 equiv), 4 (1.2 equiv), Al(CH₃)₃ (4.0 equiv), TEA, toluene, reflux, 16 h. (c) NaI, CuI, N1,N2-dimethylethanediamine, 1,4-dioxane, 110 °C. (d) Ethynyltrimethylsilane, Pd(PPh₃)₂Cl₂, CuI, 1,4-dioxane, rt, 24 h followed by TBAF, THF, rt, 2 h; (e) CF₃SO₃⁻S-(CF₃)(Ph)₂, Cu, DMF, 60 °C, 18 h; (f) PhB(OH)₂, PdCl₂(dbpf), K₂CO₃, DME:H₂O:EtOH (5:2.5:1), microwave, 110 °C, 20 min.

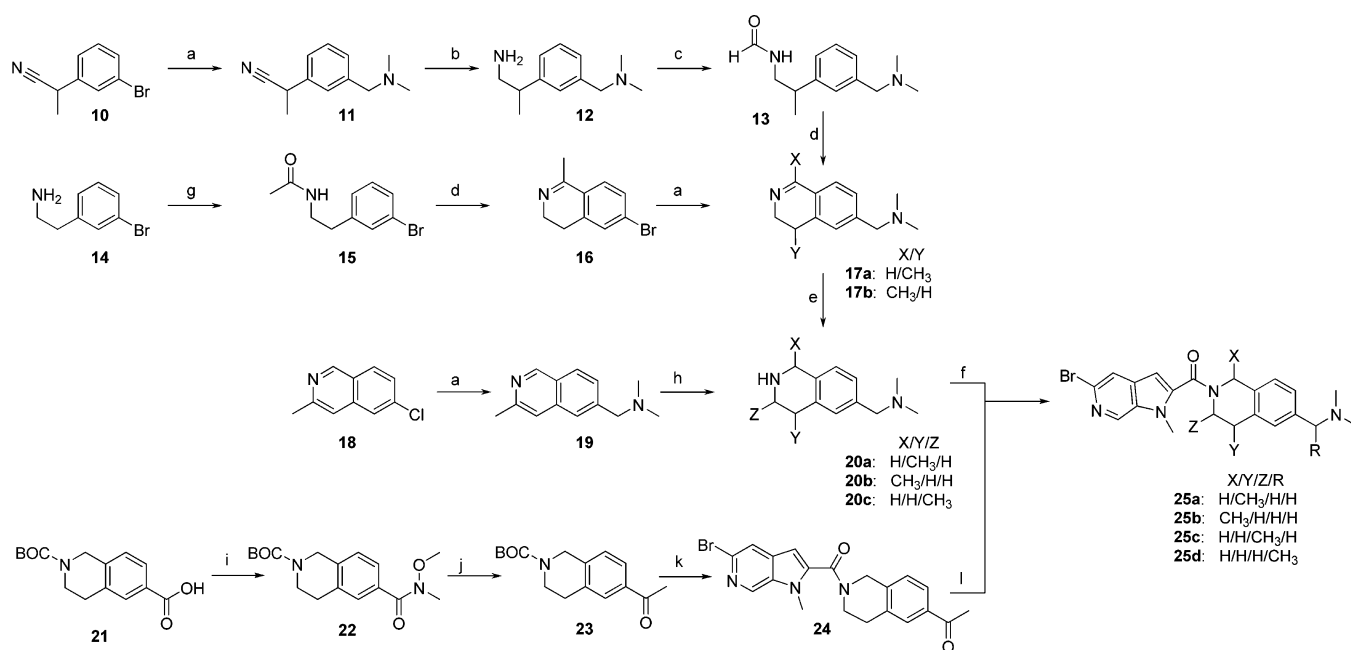
from commercially available ethyl esters (6a–6d). The N-methylated pyrrolo[2,3-c]pyridines (7a–7d) were prepared from the ethyl esters (6a–6d) by treatment with CH₃I. Palladium- or copper-catalyzed coupling reactions were utilized to introduce iodo, acetylene, trifluoromethyl, and phenyl substituents in the 5-position of the pyrrolo[2,3-c]pyridine ring. The iodo functionality (8a) was introduced by reacting the bromo-substituted ester (7c) with sodium iodide using copper(I) iodide as catalyst together with N,N-dimethylethylene-1,2-diamine.^{25,26}

Acetylene was introduced, starting from 8a, using a catalytic system of Pd(PPh₃)₂Cl₂ and copper(I) iodide reacting with ethynyltrimethylsilane as first described by Sonogashira.²⁷ The TMS group was cleaved using TBAF to give 8b. To generate the trifluoromethyl-substituted pyrrolo[2,3-c]pyridine (8c), compound 8a was treated with copper and diphenyl-(trifluoromethyl)sulfonium trifluoromethanesulfonate in DMF.²⁸ The phenyl analogue 8d was synthesized by a standard Suzuki–Miyaura coupling from the phenylboronic acid and 8a.²⁹

The esters were hydrolyzed to the acids, and the final products of 5-substituted 1-methylpyrrolo[2,3-c]pyridine-2-carboxamides (9a, 9c, 9d, 9f, and 9g) were synthesized from the corresponding acids (7a, 7c, 7d, 8b, and 8c) and the THIQ dimethylmethylene amine (4) using a standard TBTU amide coupling.³⁰ An alternative amide formation was used to make 9b and 9h, where the esters (7b and 8d) were treated with trimethylaluminum and triethylamine (TEA) and reacted with 4.³¹

To map the available space in the receptor covered by the THIQ part of compound 9c, a methyl group³² was introduced

Scheme 3. Synthesis of 5-Bromo-1-methylpyrrolo[2,3-*c*]pyridine-2-carboxamide Derivatives Comprising Aliphatic Methyl Substitutions on the THIQ Dimethylmethylene Amine^a



^aReagents: (a) $(\text{CH}_3)_2\text{NCH}_2\text{BF}_3^-\text{K}^+$, $\text{Pd}(\text{OAc})_2$, S-Phos, K_3PO_4 , 1,4-dioxane:H₂O, 100 °C. (b) H₂, Raney-Ni, MeOH. (c) HCOCH_3 , rt, 4.5 h. (d) $(\text{COCl})_2$, FeCl_3 , DCM, -78 to 25 °C. (e) NaBH_4 , MeOH. (f) 5-Bromo-1-methyl-pyrrolo[2,3-*c*]pyridine-2-carboxylic acid (from hydrolysis of 7c) EDC, HOBT, TEA, DMF, 25 °C, 3 h. (g) CH_3COCl , pyridine:DCM (1:1), 2 h, 25 °C; (h) H₂, PtO_2 , HCl, MeOH. (i) Ghosez reagent, Weinreb amine, TEA, DCM, rt, 14 h. (j) CH_3MgCl , THF, rt, 1 h. (k) 10% TFA in DCM, followed by T3P, TEA, EtOAc, 0 to 60 °C. (l) MeNH_2 in EtOH, NaBH_4 , rt to 50 °C followed by formaldehyde (aq), $\text{NaBH}(\text{OAc})_3$.

in all aliphatic positions of the THIQ (**25a–25d**) (see Scheme 3). The syntheses of the different THIQ analogues followed two principal routes, where the THIQ scaffold was either built up from a phenethylamine analogue (**10** or **14**) or from the aromatic isoquinoline **18** (Scheme 3). The first step in the synthesis of **20a** was to react the commercial building block 2-(3-bromophenyl)propanenitrile with dimethylaminomethyltrifluoroborate using a palladium-catalyzed Suzuki–Miyaura protocol to give **11**.³³ The nitrile in **11** was reduced using Raney-nickel and hydrogen gas to give the amine (**12**), which was formylated in neat methyl formate to give **13**. The intramolecular condensation of compound **13** to give **17a** was conducted using oxalyl chloride and FeCl_3 .³⁴ All attempts to form the THIQ using polyphosphoric acid or *p*-toluenesulfonic acid³⁵ were unsuccessful. The imine **17a** was reduced using sodium borohydride to form the THIQ **20a**.

Synthesis of **20b** started from the commercially available phenethylamine **14** that was acetylated using acetyl chloride to give **15**. Compound **15** was then treated with FeCl_3 and oxalyl chloride to form the ring **16**.³⁴ The methylene-dimethylamine was introduced as above with a Suzuki–Miyaura coupling on the bromide **16**,³³ and the imine was reduced to give **20b** using sodium borohydride in the same way as described for **13**.

Starting from the aromatic isoquinoline **18**, compound **20c** was accomplished by introduction of methylene-dimethylamine via a Suzuki–Miyaura coupling on the chloride to give **19**.³³ To generate **20c**, the isoquinoline was reduced to THIQ by hydrogenation.

To generate the final compounds (**25a–25c**) the THIQ derivatives (**20a–20c**) were coupled to the 5-bromo-1-methylpyrrolo[2,3-*c*]pyridine-2-carboxylic acid (from hydrolysis of **7c**) using a standard EDC/HOBT amide coupling.²⁴ The

enantiomers of **25a** were separated using reversed phase chiral chromatography to give **25e** and **25f**. For synthesis of **25d**, commercially available **21** was converted to the acid chloride and treated with dimethylhydroxylamine to form the corresponding Weinreb amide (**22**).³⁶ To make the methyl ketone (**23**), the Weinreb amide was treated with methyl magnesium chloride. After Boc deprotection the amine was coupled to 5-bromo-1-methylpyrrolo[2,3-*c*]pyridine-2-carboxylic acid using a standard T3P coupling,³⁷ giving compound **24**. Two consecutive reductive aminations, first on the ketone using methyl amine followed by formaldehyde on the resulting secondary amine, formed the final compound **25d**.

RESULTS AND DISCUSSION

It is well-established that high lipophilicity and high molecular weight are properties that may hamper development of oral drugs.³⁸ To address liabilities profiled in **1**, alternatives to the indole scaffold were explored in a designed set of 177 compounds (Scheme 1). For all compounds synthesized, the *in vitro* functional activity in a GPR103 inositol-1-phosphate (IP-1) assay and $\log D_{7.4}$ were measured. LLE was calculated according to eq 1.³⁹ A higher LLE may indicate less lipophilic contribution to potency and is therefore a suitable way to identify lead compounds with specific receptor interactions.³⁹ In Figure 3, 45 compounds with confirmed GPR103 antagonist activity are shown.

$$\text{LLE} = \text{pIC}_{50} - \log D_{7.4} \quad (1)$$

Three compounds with antagonistic activity below 1 μM and lipophilicity in the range of $0.5 < \log D_{7.4} < 2.5$ were identified. The reduced lipophilicity achieved from exchanging the indole-scaffold improved the LLE (range 5.6–4.6) compared to

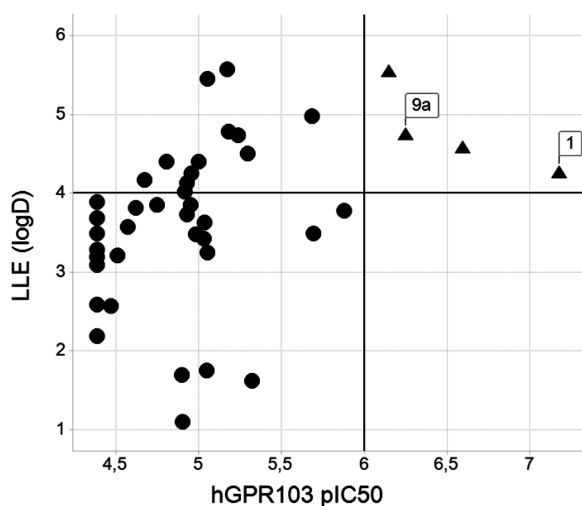


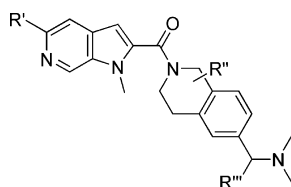
Figure 3. GPR103 pIC₅₀ vs LLE³⁹ displaying identification of three new scaffolds (marked as ▲) to explore in lead identification.

compound **1** (LLE = 4.3). Among the newly identified compounds, 1-methylpyrrolo[2,3-*c*]pyridine-2-carboxamide **9a** with LLE = 4.8 was selected as the indole replacement suitable for further exploration. A variety of regioisomers of 1-methylpyrrolo[2,3-*c*]pyridine-2-carboxamide were part of the initial library, and SAR assessment suggested that the substitution at the 5-position and the pyridine nitrogen in the 6-position were crucial for potency (data displayed in Figure 3, structures not shown). Therefore, further exploration was focused on the 5-position of the pyrrolo[2,3-*c*]pyridine to enhance potency and explore size restrictions.

Data from functional assessment of GPR103 antagonism and log $D_{7.4}$ measurements are shown in Table 1. Halogenation in the 5-position of the pyrrolo[2,3-*c*]pyridine as in compounds **9a**, **9c**, and **9e** gave an increase in antagonistic effect on GPR103 compared to the unsubstituted **9b**. With substitution of the halogen with a methyl substituent (compound **9d**), the potency decreased 100-fold compared to **9c**. For larger substituents, such as alkyne (**9f**) and trifluoromethyl (**9g**), the potency dropped approximately 10 times, and phenyl (**9h**) was not tolerated at all. From calculated $pK_{a,calcd}$ values it is speculated that electronic properties of the pyrrolo[2,3-*c*]pyridine nitrogen could be of importance for antagonistic activity (5-chloro substitution, $pK_{a,calcd} = 2.9$; 5-bromo-substitution, $pK_{a,calcd} = 4.1$; 5-hydrogen-substitution, $pK_{a,calcd} = 6.6$; 5-methyl substitution, $pK_{a,calcd} = 7.1$). Compound **9c** was further evaluated when exploring SAR of the THIQ with a set of compounds introducing a methyl group in all aliphatic positions.³² These analogues were initially screened as racemates. Methyl substitution in the 1- and 3-positions (**25b**, **25c**), as well as on the methylene linker in the 6-position of the THIQ (**25d**), gave compounds equipotent to **9a**. The racemate **25a** was 5 times more potent than **9a**. Separation of the enantiomers of **25a** identified **25e** with a measured IC₅₀ of 46 nM compared to enantiomer **25f** (IC₅₀ = 870 nM).

During the course of compound exploration, compounds were further profiled for DMPK and safety properties. Data for **1**, **9c**, and **25e** are shown in Table 2. In general, the change from the indole to the pyrrolo[2,3-*c*]pyridine scaffold lowered the log $D_{7.4}$ about 1.5 units and led to a decrease in intrinsic clearance corrected for incubational binding in both human hepatocytes and human liver microsomes. Metabolism identification in human liver microsome incubations on indole

Table 1. SAR of Position 5 of the Pyrrolo[2,3-*c*]pyridines and Methylation in the THIQ Substructure



compd	R'	R''	R'''	log $D_{7.4}$ ^a	<i>h</i> GPR103 IP-1 IC ₅₀ (μM) ^b
9a	Cl	H	H	1.5 (1)	0.57 ± 0.09 (2)
9b	H	H	H	0.9 ± 0 (3)	2.9 ± 0.6 (2)
9c	Br	H	H	1.7 ± 0.2 (3)	0.24 ± 0.08 (4)
9d	CH ₃	H	H	1.3 ± 0.1 (3)	18.9 ± 0.7 (2)
9e	I	H	H	2.0 ± 0.1 (3)	0.13 ± 0.04 (2)
9f	CCH	H	H	1.2 ± 0.1 (3)	6.0 ± 0.7 (2)
9g	CF ₃	H	H	1.8 ± 0.2 (3)	3.3 ± 0.2 (3)
9h	Ph	H	H	3.0 ± 0.1 (4)	>41 (3)
25a	Br	3-CH ₃	H	2.1 ± 0.1 (2)	0.11 ± 0.005 (2)
25b	Br	1-CH ₃	H	2.2 ± 0.1 (2)	0.5 ± 0.1 (3)
25c	Br	4-CH ₃	H	2.1 ± 0.1 (3)	0.71 ± 0.02 (2)
25d	Br	H	CH ₃	1.8 ± 0.2 (3)	0.46 ± 0.04 (5)
25e	Br	(+)-7-CH ₃	H	2.1 ± 0.1 (3)	0.046 ± 0.004 (2)
25f	Br	(-)-7-CH ₃	H	1.9 ± 0.3 (3)	0.88 ± 0.017 (2)

^aValues are reported as a single measurement, or where more than one independent experiment was done, the mean ± SD is given with the number of independent experiments (*N*) in parentheses. ^bIC₅₀ is reported as mean ± SD with the number of experiments (*N*) in parentheses. The confidence interval ratio (CIR) was 2.0 for the *h*GPR103 IP-1 assay with minimum discriminatory ratio (MDR) of 2.8. The 95% confidence interval for the true IC₅₀ of the compound is the single calculated value of IC₅₀ ×/÷ CIR. Two compounds are considered different if their IC₅₀ differ by a ratio >MDR (*p* = 0.05).

Table 2. DMPK Properties and Cardiac Safety Profile for Selected Compounds

assay	1	9c	25e
<i>h</i> GPR103 IP-1 IC ₅₀ (μM) ^a	0.07 ± 0.02 (52)	0.24 ± 0.08 (4)	0.046 ± 0.004 (2)
<i>h</i> GPR103 RLB IC ₅₀ (μM) ^a	0.07 ± 0.02 (5)	0.28 ± 0.02 (4)	0.04 ± 0.02 (2)
<i>m</i> GPR103A IP-1 IC ₅₀ (μM) ^a	0.09 ± 0.02 (7)	0.33 ± 0.08 (5)	0.058 (1)
<i>m</i> GPR103B IP-1 IC ₅₀ (μM) ^a	0.08 ± 0.02 (7)	0.10 ± 0.01 (5)	0.015 (1)
log <i>D</i> _{7,4} ^b	3.0 ± 0.1 (3)	1.7 ± 0.2 (3)	2.1 ± 0.1 (3)
solubility (μM) ^b	62 ± 10 (3)	>1000 (2)	>1000 (2)
intrinsic clearance in vitro in human hepatocytes (μL/min/10 ⁶ cells) ^c (CIR = 1.4)	40 ± 3 (3)	5.3 ± 0.9 (3)	6.0 ± 0.6 (3)
intrinsic clearance in vitro in human liver microsomes (μL/min/mg) ^c (CIR = 1.7)	156 ± 22 (3)	16 ± 2 (3)	26 ± 5 (3)
Caco-2 apparent permeability (10 ⁻⁶ cm/s) ^b	7.8 (1)	13.2 (1)	11.8 (1)
CYP inhibition (IC ₅₀ 2D6) (μM) ^b	2.9 ± 0.8 (2)	>20 (2)	>20 (3)
<i>h</i> ERG IC ₅₀ (μM) ^d	4.9 ± 1.7 (2)	31.2 (1)	12.9 (1)
<i>h</i> Nav1.5 IC ₅₀ (μM) ^d	10.3 (1)	>33 (1)	>33 (3) ^e
<i>h</i> IKs IC ₅₀ (μM) ^d	10.5 (1)	>33 (1)	>33 (1) ^e

^aIC₅₀ is reported as mean ± SD with the number of experiments (*N*) in parentheses. The confidence interval ratio (CIR) is reported as a statement of the assay quality. The 95% confidence interval for the true IC₅₀ of the compound is the single calculated value of IC₅₀ ×/÷ CIR. *h*GPR103 IP-1 CIR = 2.0; *h*GPR103 RLB CIR = 1.7. The minimum discriminatory ratio (MDR) for the IP-1 assay was 2.8 and MDR = 2.1 for the radioligand binding assay. Two compounds are considered different if their IC₅₀ differ by a ratio >MDR (*p* = 0.05). ^bValues are reported as a single measurement, or where more than one independent experiment was done, the mean ± SD is given with the number of independent experiments (*N*) in parentheses. ^cMeasured intrinsic clearance corrected for unspecific binding in incubations. ^dIC₅₀ is reported as mean ± SD with the number of experiments (*N*) in parentheses. Experiments were run using four replicates at each concentration. The confidence interval ratio (CIR) is reported as a statement of the assay quality. The 95% confidence interval for the true IC₅₀ of the compound is the single calculated value of IC₅₀ ×/÷ CIR. *h*ERG CIR = 2.0; *h*Nav1.5 CIR = 2.0; *h*IKs CIR = 2.3. ^eMeasured for the racemate 25a.

and pyrrolo[2,3-*c*]pyridine compounds revealed that the major metabolites were the same for the two scaffolds (data not shown). Hence, the improved metabolic stability was correlated to the structural modification and was not a consequence of altered metabolic pathways. Compounds 9c and 25e displayed no inhibition toward any of the six tested isoforms of cytochrome P450 enzymes (CYP3A4, CYP1A2, CYP2D6, CYP2C8, CYP2C9, and CYP2C19) in a high-throughput fluorescence assay. The solubility was dramatically increased and, in combination with the high apparent permeability measured in an in vitro Caco-2 assay, the novel compounds are expected to have a high fraction absorbed in vivo. Improved physicochemical properties accomplished with the pyrrolo[2,3-*c*]pyridine scaffold also increased margins to cardiac liability targets such as *h*ERG, human cardiac sodium channel 1.5 (*h*Nav1.5), and human cardiac slowly activating delayed rectifier K⁺ channel (*h*IKs) (Table 2). Investigated compounds 1, 9c, and 25e were confirmed to bind human GPR103 using a radioligand binding assay (RLB). Species crossover was confirmed in mouse GPR103A and B IP-1 assays, which showed that both compounds 9c and 25e had similar potency range in mouse compared to human GPR103, but that they were slightly more potent on *m*GPR103B (3.3 and 3.8 times respectively) compared to *m*GPR103A.

To investigate the ability of a GPR103 antagonist to modulate appetite, obese female mice on a high-fat diet were administered 25e by oral gavage during automated food intake measurement (FIA). The study was initiated with four basal acclimatization days in the FIA monitoring system, measuring food intake and meal frequency. Once acclimatized, mice were given either vehicle or 25e at 75 and 125 μmol/kg twice daily (BID) for 3 days, with continuous measurements on the food intake and meal frequency. As shown in Figure 4, animals treated with 25e reduced their food intake compared to vehicle treated animals in a dose-dependent manner. The highest dose (125 μmol/kg) gave a significant reduction of 86% (*p* < 0.001) in cumulative food intake compared to vehicle-treated animals at day 3. Treatment with 25e did not change the eating pattern

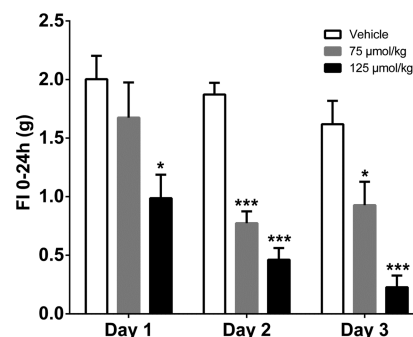


Figure 4. Compound 25e administered by oral gavage at 75 μmol/kg BID (gray bars, *N* = 8) and 125 μmol/kg BID (black bars, *N* = 7) decreased food intake dose dependently in obese C57Bl/6 mice, but vehicle (*N* = 8) did not. Results are presented as cumulative food intake in grams over 24 h periods for 3 days. Data are presented as mean ± SEM, **p* < 0.05, ****p* < 0.001.

compared to vehicle-treated animals, indicating that GPR103 antagonist 25e reduces appetite without introducing malaise. Also, an indication of body weight reduction was observed in the compound-treated animals, but the duration of the study was too short to show significance in body weight reduction (Supporting Information, Supplementary Figure S9).

Data from [¹²⁵I]QRFP43 binding studies suggest that the antagonists presented in this paper are competitive with the endogenous agonist. To elucidate the bioactive pharmacophore, the free solution structure of QRFP26_(20–26) was determined using a methodology specifically designed to characterize flexible systems⁴⁰ and was compared to compound 9c. Overall, QRFP26_(20–26) exhibited a high degree of conformational flexibility in solution (Figure 5A), consistent with a previous study.¹³

Moreover, the detailed experimental results show that the peptide backbone mainly adopts an extended (β -strand-like) conformation that accounts for 60% of the conformations observed in solution (Figure 5B). No other single backbone

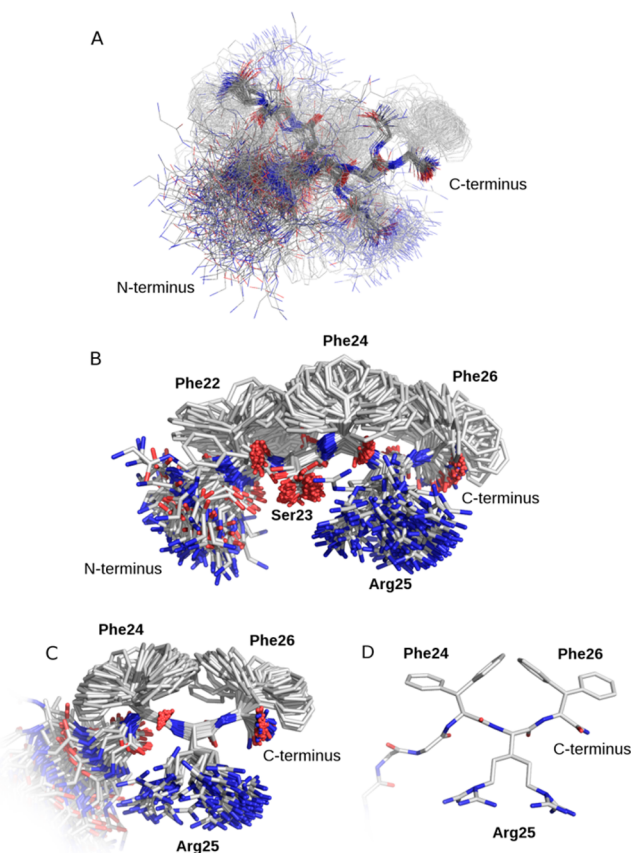


Figure 5. (A) Main structure overview, showing the complete ensemble generated. The peptide backbone is highlighted in dark gray for clarity. The overlay is on the backbone of Ser23, and the additional flexibility of the N-terminal glycines can be seen. (B) The dominant overall shape of the molecule as determined by the dominant backbone conformation. This shows the overall amphiphilic pattern of the molecule and the relatively well-defined gross shape. (C) Overlay focusing on the key C-terminal residues and their most dominant conformational families. (D) Idealized conformations representing the dominant conformational families (macrostates) of the key C-terminal residues.

conformation accounts for more than 20% of the conformations, and most of them are much less common. With the backbone in the dominant extended β -strand-like conformation, the hydrophobic Phe22, Phe24, and Phe26 side chains group together on one side of the molecule while the hydrophilic Ser23 and Arg25 residues sit on the opposite side (Figure 5B). The second most populated backbone conformations are those in which single residues adopt a conformation in the α -helical region of the Ramachandran plot (Supporting Information, Supplementary Figure S4). Conformations with multiple residues in α -helix-like conformations are rare (<2% of the ensemble): there is no evidence of incipient helix formation in the peptide. The N-terminal glycine residues adopt largely extended conformations and are less ordered than the rest of the molecule. All three phenylalanine side chains are best described by a mixture of two staggered rotamers at χ_1 and adopt conformations close to orthogonal at χ_2 (Supporting Information, Supplementary Figure S5). The side chain of Arg25 adopts a large number of conformations, but four extended conformations account for approximately 90% of the conformations observed in solution

(these consist of two staggered rotamers at χ_1 , extended trans rotamers at χ_2 and χ_3 , and two approximately orthogonal rotamers at χ_4 ; Supporting Information, Supplementary Figure S5). Full details describing the conformational parameters for each rotatable bond are given in the Supporting Information (Supplementary Table S9). Recently, the first structural study of QRFP26_(20–26) conformation by NMR was published by Pierry et al.⁴¹ The data presented in this publication differ from our findings. We observed a number of pieces of data that are clearly incompatible with a substantial helical content in the structural ensemble (scalar couplings, diagnostic NOE patterns), whereas they report helix or helixlike secondary structure. In particular, the diagnostic medium intensity $\alpha, N(i, i + 3)$ NOE crosspeak between residues 22 and 25, which is shown in their Figure 6, is clearly absent in our own NOESY spectrum. The source of the difference could lie in their use of DPC micelles, whereas the study presented in this paper was performed in aqueous solution. DPC micelles are commonly seen to induce secondary structures in short peptides, due to the requirement of burying hydrophilic moieties in a hydrophobic environment.

For the three key C-terminal amino acid residues¹¹ of QRFP26_(20–26), eight dominant conformational families in solution were found (Figure 5C), and we hypothesize that the bioactive conformation of the peptide lies within this set of conformations.^{40,42} These eight conformational families were simplified by setting each torsion to its mean position, leaving eight idealized peptide conformations (Figure 5D) for comparison with low-energy conformations of **9c**. An excellent overlay of key pharmacophore features of the terminal Arg-Phe-NH₂ in QRFP26_(20–26) and **9c** was observed (Figure 6) using

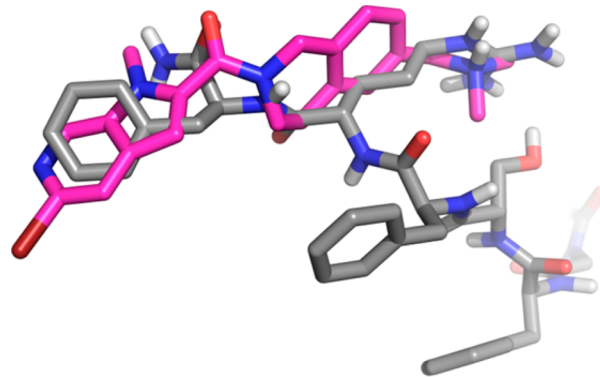


Figure 6. Structural overlay of one of the idealized conformations of QRFP26_(20–26) (gray carbons) and a low-energy conformation of **9c** (magenta carbons). Pharmacophore features including the aromatic ring plane, the Phe26 carbonyl oxygen, and the positively charged Arg25 side chain were captured by the ligand, in addition to the overall shape envelope of the two C-terminal amino acids.

one of the most populated conformations of the agonist peptide. This conformation of compound **9c** used in this overlay was found to be 0.8 kcal/mol higher than the lowest energy conformation identified after optimization with quantum mechanics and was considered a reasonable conformation consistent with the current understanding of modeling energy calculations. Specifically, the relationship of the positively charged amine, the aromatic pyrrolo[2,3-*c*]pyridine, and the central carbonyl moieties of the antagonist closely matched the relationship of the Arg25 and Phe26 side chains and the C-terminal amide carbonyl of the agonist. It is

known that small structural differences can make an agonist into an antagonist (and vice versa) and that both agonists and antagonists can share common pharmacophore motifs.^{43–45} The harmony between these scaffolds is suggestive that the presently described compounds and QRFP26_(20–26) bind with overlapping pharmacophores and that the selected conformation of the peptide may be similar to the bioactive.

CONCLUSIONS

In summary, we have reported the development and synthesis of a series of GPR103 small molecule antagonists with lead compounds demonstrating DMPK and safety properties amenable to drug development. Drivers for lipophilicity were identified within the indole motif and, through replacement with pyrrolo[2,3-*c*]pyridine, lead compounds with increased metabolic stability and solubility as well as improved margins to CYP inhibition and cardiac liability targets were achieved. We also report unique preclinical data on the anorexigenic efficacy of a GPR103 antagonist. Compound **25e** demonstrated a significant and dose-dependent reduction on food intake compared to vehicle-treated animals as assessed in a 3 day automated food intake measurement study.

To support further design on GPR103 antagonists, the free solution structure of the C-terminal motif of the endogenous GPR103 ligand QRFP26 was studied using the heptapeptide QRFP26_(20–26). The solution structure of QRFP26_(20–26) exhibited a high degree of conformational flexibility, in which the peptide backbone mainly adopted an extended conformation where the overall placement of the amino acid side chains gave the peptide an amphiphilic character. Considering the NMR data in combination with conformational studies on the antagonists, we were able to elucidate that QRFP26_(20–26) and this class of GPR103 antagonists could share overlapping pharmacophores and may be able to bind accordingly. We therefore hypothesize that the selected C-terminal conformation of the peptide is similar to the bioactive one and that the synthesized antagonists mimic the C-terminal Arg25-Phe26 residues of the endogenous ligand.

EXPERIMENTAL SECTION

General Description. ¹H NMR spectra were recorded on a Bruker Avance II or III spectrometer at a proton frequency of 300, 400, 500, or 600 MHz at 25 °C, with the frequency stated for each experiment. The chemical shifts (δ) are reported in ppm and referenced indirectly to TMS via the solvent signals (CDCl₃ at 7.26 ppm, DMSO-*d*₆ at 2.50 ppm, CD₃OD at 3.31 ppm). All microwave-assisted synthesis was carried out in an Initiator synthesizer single mode cavity instrument producing controlled irradiation with a power range 0–400 W at 2450 MHz (Biotage AB, Uppsala, Sweden). UHPLC–MS experiments were performed using a Waters Acquity UHPLC system combined with a SQD mass spectrometer. The UHPLC system was equipped with both a BEH C₁₈ column (1.7 μ m, 2.1 \times 50 mm) in combination with a 46 mM (NH₄)₂CO₃/NH₃ buffer at pH 10 and a HSS C₁₈ column (1.8 μ m, 2.1 \times 50 mm) in combination with 10 mM formic acid, 1 mM ammonium formate buffer at pH 3. The flow rate was 1 mL/min. The mass spectrometer used ESI \pm as the ion source. Preparative HPLC was performed by a Waters Fraction Lynx med ZQ MS detector on either a Waters Xbridge C₁₈ OBD 5 μ m column (19 \times 150 mm, flow rate 30 mL/min, or 30 \times 150 mm, flow rate 60 mL/min) using a gradient of 5–95% MeCN with 0.2% NH₃ at pH 10 or a Waters SunFire C₁₈ OBD 5 μ m column (19 \times 150 mm, flow rate 30 mL/min, or 30 \times 150 mm, flow rate 60 mL/min) using a gradient of 5–95% MeCN with 0.1 M formic acid. Molecular mass (HR-ESI-MS) was determined on a mass spectrometer equipped with an electrospray ion source. Column chromatography was performed on a Biotage system

using a SiO₂ column with UV detection. LC/MS/MS for DMPK and physicochemical assays were performed on an Agilent HPLC 1100 series binary pump and a CTC injector in combination with a Waters Quattro Premier or a Waters Acquity UPLC coupled to a Waters Micromass TQD. The columns used were either an Atlantis T3 C₁₈ (3 μ m, 2.1 \times 30 mm) or an Acquity UPLC HSS T3 C₁₈ (1.8 μ m, 2.1 \times 50 mm). Gradient elution was used with MeCN/H₂O containing 0.2% formic acid. Purity of all test compounds was determined by LC/MS. All screening compounds had purity >95%.

Ethyl 5-Chloro-1-methyl-1H-pyrrolo[2,3-*c*]pyridine-2-carboxylate (7a). Compound **6a** (1.60 g, 7.14 mmol), iodomethane (0.53 mL, 8.56 mmol), and cesium carbonate (3.0 g, 9.28 mmol) were mixed in DMF (20 mL) under N₂, and the reaction mixture was stirred for 16 h at rt. The crude product was precipitated by addition of H₂O (200 mL). The solid was filtered, washed with H₂O, and then dissolved in DCM. The organic solution was washed with H₂O, separated, and concentrated to yield **7a** (1.44 g, 84%) as a yellow solid. ¹H NMR (500 MHz, DMSO-*d*₆): δ 1.35 (t, *J* = 7.1 Hz, 3H), 4.11 (s, 3H), 4.36 (q, *J* = 7.1 Hz, 2H), 7.23 (s, 1H), 7.76 (s, 1H), 8.90 (s, 1H). MS (ESI) *m/z* [M + H]⁺: 239.1.

Ethyl 1-Methyl-1H-pyrrolo[2,3-*c*]pyridine-2-carboxylate (7b). This compound was synthesized using the protocol as described for **7a**. Compound **6b** (150 mg, 0.79 mmol) was used in the reaction. Instead of precipitation, the solvent was evaporated and the residue was purified by preparative HPLC using basic conditions to yield **7b** (32 mg, 20%). ¹H NMR (500 MHz, DMSO-*d*₆): δ 1.35 (t, *J* = 7.1 Hz, 3H), 4.13 (s, 3H), 4.36 (q, *J* = 7.1 Hz, 2H), 7.26 (d, *J* = 0.9 Hz, 1H), 7.64 (dd, *J* = 0.9, 5.5 Hz, 1H), 8.22 (d, *J* = 5.5 Hz, 1H), 9.06 (s, 1H). MS (ESI) *m/z* [M + H]⁺: 205.2.

Ethyl 5-Bromo-1-methyl-1H-pyrrolo[2,3-*c*]pyridine-2-carboxylate (7c). This compound was synthesized using the protocol as described for **7a**. Compound **6c** (992 mg, 3.69 mmol) was used to yield **7c** (965 mg, 92%) as a yellow solid. ¹H NMR (400 MHz, DMSO-*d*₆): δ 1.33 (t, *J* = 7.1 Hz, 3H), 4.08 (s, 3H), 4.34 (q, *J* = 7.1 Hz, 2H), 7.19 (d, *J* = 0.8 Hz, 1H), 7.88 (d, *J* = 0.8 Hz, 1H), 8.87 (s, 1H). MS (ESI) *m/z* [M + H]⁺: 284.8.

Ethyl 1,5-Dimethyl-1H-pyrrolo[2,3-*c*]pyridine-2-carboxylate (7d). Sodium hydride (17 mg, 0.40 mmol) was added to a solution of **6d** (82 mg, 0.40 mmol) in dry DMF (5 mL) under N₂ at rt. After being stirred for 30 min, iodomethane (0.025 mL, 0.40 mmol) dissolved in dry DMF (1 mL) was added dropwise. The reaction mixture was stirred for 16 h at rt under N₂. The solvent was removed and the crude was used as such in the next step. MS (ESI) *m/z* [M + H]⁺: 219.1.

Ethyl 5-Iodo-1-methyl-1H-pyrrolo[2,3-*c*]pyridine-2-carboxylate (8a). A mixture of **7c** (1.08 g, 3.81 mmol), copper(I) iodide (0.15 g, 0.76 mmol), N₁,N₂-dimethylethane-1,2-diamine (0.082 mL, 0.76 mmol), and sodium iodide (1.14 g, 7.63 mmol) in 1,4-dioxane (17.5 mL) was added to a microwave vial, which was flushed with N₂ and sealed. The reaction mixture was heated at 110 °C in an oil bath for 72 h. The reaction mixture was then diluted with DCM (20 mL) and filtered through a pad of Celite, and the filtrate was concentrated. The residue was purified by automated flash chromatography using a gradient of 0–40% of EtOAc in heptane as mobile phase to yield **8a** (1.02 g, 81%). ¹H NMR (500 MHz, DMSO-*d*₆): δ 1.34 (t, *J* = 7.1 Hz, 3H), 4.09 (s, 3H), 4.36 (q, *J* = 7.1 Hz, 2H), 7.19 (d, *J* = 0.8 Hz, 1H), 8.12 (d, *J* = 0.8 Hz, 1H), 8.89 (s, 1H). MS (ESI) *m/z* [M + H]⁺: 331.1.

Ethyl 5-Ethynyl-1-methyl-1H-pyrrolo[2,3-*c*]pyridine-2-carboxylate (8b). N-Ethyl-N-isopropylpropan-2-amine (0.129 mL, 0.74 mmol) was added to a mixture of **8a** (163 mg, 0.49 mmol), bis(triphenylphosphine)palladium(II) chloride (35 mg, 0.05 mmol), and copper(I) iodide (9 mg, 0.05 mmol) in 1,4-dioxane (9 mL) under N₂. The reaction mixture was purged with N₂ for 5 min. Ethynyltrimethylsilane (0.106 mL, 0.74 mmol) was added dropwise and the color of the reaction mixture changed from light yellow to dark blue to brown. The resulting reaction mixture was stirred at rt for 24 h under N₂. The reaction mixture was poured into H₂O and extracted with EtOAc (3 \times). The combined organic layers were washed with brine, dried over MgSO₄, filtered, and concentrated in vacuo. The residue was purified by automated flash chromatography using a

gradient of 5–40% of EtOAc in heptane as mobile phase to yield ethyl 1-methyl-5-((trimethylsilyl)ethynyl)-1*H*-pyrrolo[2,3-*c*]pyridine-2-carboxylate (88 mg, 59%). ¹H NMR (500 MHz, DMSO-*d*₆): δ 0.25 (s, 9H), 1.35 (t, *J* = 7.1 Hz, 3H), 4.13 (s, 3H), 4.36 (q, *J* = 7.1 Hz, 2H), 7.26 (s, 1H), 7.87 (d, *J* = 1.1 Hz, 1H), 9.02 (s, 1H). MS (ESI) *m/z* [M + H]⁺: 301.1.

A 1 M TBAF solution in THF (0.337 mL, 0.34 mmol) was added dropwise to a solution of ethyl 1-methyl-5-((trimethylsilyl)ethynyl)-1*H*-pyrrolo[2,3-*c*]pyridine-2-carboxylate (88 mg, 0.29 mmol) in THF (1 mL) at rt under N₂ and the reaction mixture was stirred for 2 h. The reaction mixture was treated with NH₄Cl solution (sat. aq, 5 mL) and extracted with EtOAc (3×). The combined organic layers were washed with H₂O and brine, dried over Mg₂SO₄, filtered, and concentrated. The residue was purified by automated flash chromatography using a gradient of 30–50% of EtOAc in heptane as mobile phase to yield **8b** (62 mg, 93%) as a white solid after evaporation of the solvent. ¹H NMR (500 MHz, DMSO-*d*₆): δ 1.35 (t, *J* = 7.1 Hz, 3H), 4.08 (s, 1H), 4.13 (s, 3H), 4.36 (q, *J* = 7.1 Hz, 2H), 7.27 (s, 1H), 7.88 (d, *J* = 1.0 Hz, 1H), 9.04 (s, 1H). MS (ESI) *m/z* [M + H]⁺: 209.3.

Ethyl 1-Methyl-5-(trifluoromethyl)-1*H*-pyrrolo[2,3-*c*]pyridine-2-carboxylate (8c). Copper (89 mg, 1.40 mmol) was added to a solution of diphenyl(trifluoromethyl)sulfonium trifluoromethanesulfonate (377 mg, 0.93 mmol) and **8a** (154 mg, 0.47 mmol) in DMF (4.7 mL) under N₂ in a microwave vial. The vial was sealed and stirred at 60 °C for 18 h. The reaction mixture was cooled down to rt, diluted with EtOAc, and washed with H₂O (3×). The combined organic layers were washed with brine, dried over Na₂SO₄, filtered, and concentrated. The residue was purified by automated flash chromatography using a gradient of 0–35% of EtOAc in heptane as mobile phase to yield **8c** (102 mg, 80%). ¹H NMR (500 MHz, DMSO-*d*₆): δ 1.36 (t, *J* = 7.1 Hz, 3H), 4.19 (s, 3H), 4.39 (q, *J* = 7.1 Hz, 2H), 7.43 (s, 1H), 8.23 (s, 1H), 9.21 (s, 1H). ¹⁹F NMR (470 MHz, DMSO-*d*₆): δ –64.44 (s).

Ethyl 1-Methyl-5-phenyl-1*H*-pyrrolo[2,3-*c*]pyridine-2-carboxylate (8d). Compound **8a** (120 mg, 0.36 mmol), phenylboronic acid (58 mg, 0.47 mmol), 1,1'-bis(*di-tert*-butylphosphino)ferrocene palladium (Pd-118) (23 mg, 0.04 mmol), and potassium carbonate (50 mg, 0.36 mmol) were mixed with DME (2.5 mL), H₂O (1.25 mL), and EtOH (absolute, 99.5%, 0.5 mL) in a microwave vial under N₂. The mixture was flushed with N₂, sealed, and heated under microwave irradiation at 110 °C for 20 min. The mixture was diluted with DCM (10 mL), filtered and the solvent evaporated. The residue was purified by preparative HPLC using acidic conditions to yield **8d** (42 mg, 41%). ¹H NMR (500 MHz, DMSO-*d*₆): δ 1.36 (t, *J* = 7.1 Hz, 3H), 4.16 (s, 3H), 4.38 (q, *J* = 7.1 Hz, 2H), 7.30 (d, *J* = 0.8 Hz, 1H), 7.34–7.39 (m, 1H), 7.47 (t, *J* = 7.7 Hz, 2H), 8.08 (d, *J* = 1.1 Hz, 1H), 8.10 (d, *J* = 1.3 Hz, 1H), 8.20 (d, *J* = 1.1 Hz, 1H), 9.14 (s, 1H). MS (ESI) *m/z* [M + H]⁺: 281.1.

General Coupling Method A. 2-(1*H*-Benzo[*d*][1,2,3]triazol-1-yl)-1,1,3,3-tetramethylisouronium tetrafluoroborate (TBTU, 1.1 equiv) was added to a solution of 5-substituted-1-methyl-1*H*-pyrrolo[2,3-*c*]pyridine-2-carboxylic acid (1 equiv), **4** (1.01 equiv), and *N*-ethyl-*N*-isopropylpropan-2-amine (4 equiv) in DMF (*c* = 0.2 M) at rt under N₂. After being stirred for 18 h, the reaction mixture was poured into NaHCO₃ (sat. aq) solution and was extracted with DCM (3×). The combined organic layers were washed with brine, dried through a phase separator, and concentrated. The residue was purified by preparative HPLC using basic conditions.

General Coupling Method B. Trimethylaluminum (2 M) in toluene (4 equiv) was added to a solution of ethyl 1-methyl-5-substituted-1*H*-pyrrolo[2,3-*c*]pyridine-2-carboxylate (1 equiv), *N,N*-dimethyl-1-(1,2,3,4-tetrahydroisoquinolin-6-yl)methanamine dihydrochloride (1.2 equiv), and TEA (6 equiv) in toluene (*c* = 0.06 M) under N₂ at rt. After being refluxed for 16 h, the reaction mixture was poured into H₂O and extracted with DCM (3×). The combined organic layers were washed with brine, dried, filtered, and concentrated. The residue was purified by preparative HPLC using basic conditions. Note: NMR indicated the existence of the rotamers for all the final products, but shifts were not assigned to specific rotamers.

(5-Chloro-1-methyl-1*H*-pyrrolo[2,3-*c*]pyridin-2-yl){6-[(dimethylamino)methyl]-3,4-dihydroisoquinolin-2(1*H*)-yl}methanone (9a). In a 25 mL round-bottomed flask, **7a** (0.21 g, 0.93 mmol) and sodium hydride (0.05 mL, 1.03 mmol) were dissolved in dry DMF (3 mL) under N₂ at rt to give a yellow solution. After being stirred for 1 h, iodomethane (0.058 mL, 0.93 mmol) was added and the reaction was continued for 2 h. LC/MS indicated remaining starting material. Additional sodium hydride (0.024 mL, 0.93 mmol) was added and after being stirred for 30 min, additional iodomethane (0.058 mL, 0.93 mmol) was added. The mixture was stirred for 1 h. The reaction was quenched by addition of ice and stirred for 20 min. Solvents were evaporated, and the residue was purified by preparative HPLC using acidic conditions to yield 5-chloro-1-methyl-1*H*-pyrrolo[2,3-*c*]pyridine-2-carboxylic acid (150 mg, 76%) as white solid. ¹H NMR (500 MHz, DMSO-*d*₆): δ 4.11 (s, 3H), 7.18 (s, 1H), 7.74 (s, 1H), 8.88 (s, 1H). MS (ESI) *m/z* [M + H]⁺: 211.0.

General coupling method A was used with 5-chloro-1-methyl-1*H*-pyrrolo[2,3-*c*]pyridine-2-carboxylic acid (70 mg, 0.33 mmol). The residue was purified by preparative HPLC using acidic conditions to yield **9a** (25 mg, 19%). ¹H NMR (600 MHz, DMSO-*d*₆): δ 2.14 (s, 6H), 2.85–2.98 (m, 2H), 3.30–3.40 (m, 2H), 3.66–3.99 (m, 5H), 4.61–4.95 (m, 2H), 6.67–6.88 (m, 1H), 6.96–7.33 (m, 3H), 7.68 (s, 1H), 8.79 (s, 1H). ¹H NMR indicates the existence of rotamers. HRMS (ESI) *m/z*: [M + H]⁺ calcd for C₂₁H₂₃ClN₄O 383.1638, found 383.1643.

{6-[(Dimethylamino)methyl]-3,4-dihydroisoquinolin-2(1*H*)-yl}(1-methyl-1*H*-pyrrolo[2,3-*c*]pyridin-2-yl)methanone (9b). General coupling method B was used to generate **9b** (11 mg, 8% over three steps). ¹H NMR (600 MHz, DMSO-*d*₆): δ 2.15 (s, 6H), 2.84–3.03 (m, 2H), 3.30–3.40 (m, 2H), 3.68–4.01 (m, 5H), 4.67–4.93 (m, 2H), 6.68–6.86 (m, 1H), 6.95–7.3 (m, 3H), 7.60 (d, *J* = 5.2 Hz, 1H), 8.21 (d, *J* = 5.4 Hz, 1H), 8.96 (s, 1H). HRMS (ESI) *m/z*: [M + H]⁺ calcd for C₂₁H₂₄N₄O 349.2028, found 349.2007.

(5-Bromo-1-methyl-1*H*-pyrrolo[2,3-*c*]pyridin-2-yl){6-[(dimethylamino)methyl]-3,4-dihydroisoquinolin-2(1*H*)-yl}methanone (9c). NaOH (355 mg, 8.88 mmol) was added to a solution of **7c** (710 mg, 2.51 mmol) in EtOH (absolute, 99.5%) (16 mL) and H₂O (1.6 mL). The reaction mixture was stirred for 16 h at rt before acetic acid (1.5 mL) was added to neutralize excess NaOH. The solvent was evaporated followed by addition of H₂O and then the pH was adjusted to 2–3 by addition of HCl (aq, 1 M). The precipitated solid was filtered, washed with H₂O, and dried to provide 5-bromo-1-methyl-1*H*-pyrrolo[2,3-*c*]pyridine-2-carboxylic acid (600 mg, 94%). ¹H NMR (400 MHz, DMSO-*d*₆): δ 4.08 (s, 3H), 7.15 (d, *J* = 0.8 Hz, 1H), 7.87 (d, *J* = 0.8 Hz, 1H), 8.85 (s, 1H), 13.60 (s, 1H). MS (ESI) *m/z* [M + H]⁺: 255.0.

General coupling method A was used with 5-bromo-1-methyl-1*H*-pyrrolo[2,3-*c*]pyridine-2-carboxylic acid (388 mg, 1.52 mmol). The residue was purified by preparative HPLC using basic conditions to yield **9c** (532 mg, 82%). ¹H NMR (600 MHz, DMSO-*d*₆): δ 2.14 (s, 6H), 2.85–2.98 (m, 2H), 3.30–3.40 (m, 2H), 3.64–4.01 (m, 5H), 4.57–4.93 (m, 2H), 6.68–6.88 (m, 1H), 6.94–7.36 (m, 3H), 7.76–7.98 (m, 1H), 8.70–8.90 (m, 1H). NMR indicates the existence of rotamers. HRMS (ESI) *m/z*: [M + H]⁺ calcd for C₂₁H₂₄BrN₄O 427.1133, found 427.1165.

{6-[(Dimethylamino)methyl]-3,4-dihydroisoquinolin-2(1*H*)-yl}(1,5-dimethyl-1*H*-pyrrolo[2,3-*c*]pyridin-2-yl)methanone (9d). LiOH (38 mg, 1.6 mmol) in H₂O (0.5 mL) was added dropwise to a solution of **7d** (87 mg, 0.4 mmol, crude) in EtOH (5 mL) at rt under N₂. The reaction was heated at 40 °C for 4 h. The solvent was removed and the residue 1,5-dimethyl-1*H*-pyrrolo[2,3-*c*]pyridine-2-carboxylic acid was used as such in the next step. MS (ESI) *m/z* [M + H]⁺: 191.1.

General coupling method A was used with 1,5-dimethyl-1*H*-pyrrolo[2,3-*c*]pyridine-2-carboxylic acid (76 mg, 0.4 mmol, crude). The residue was purified by preparative HPLC using basic conditions to provide **9d** (23 mg, 16%). ¹H NMR (600 MHz, DMSO-*d*₆): δ 2.15 (s, 6H), 2.82–3.00 (m, 2H), 3.30–3.40 (m, 2H), 3.69–3.98 (m, 5H), 4.66–4.92 (m, 2H), 6.58–6.77 (m, 1H), 6.93–7.32 (m, 3H), 7.41 (s, 1H), 8.81 (s, 1H). HRMS (ESI) *m/z*: [M + H]⁺ calcd for C₂₂H₂₇N₄O 363.2185, found 363.2196.

6-[(Dimethylamino)methyl]-3,4-dihydroisoquinolin-2(1H)-yl}(5-iodo-1-methyl-1H-pyrrolo[2,3-c]pyridin-2-yl)methanone (9e). A mixture of **9c** (430 mg, 1.01 mmol), copper(I) iodide (38 mg, 0.20 mmol), *N*1,*N*2-dimethylethane-1,2-diamine (0.022 mL, 0.20 mmol), and sodium iodide (302 mg, 2.01 mmol) in 1,4-dioxane (4.5 mL) in a microwave vial was flushed with N₂ and sealed. The reaction mixture was heated at 110 °C in an oil bath for 53 h. The reaction mixture was diluted with DCM (20 mL), filtered, and concentrated. The residue was purified by preparative HPLC using basic conditions to afford **9e** (380 mg, 80%). ¹H NMR (600 MHz, DMSO-*d*₆): δ 2.14 (s, 6H), 2.86–2.95 (m, 2H), 3.34–3.31 (m, 2H), 3.70–3.92 (m, 5H), 4.76 (m, 2H), 6.74 (s, 1H), 6.96–7.27 (m, 3H), 8.04 (s, 1H), 8.79 (s, 1H). HRMS (ESI) *m/z*: [M + H]⁺ calcd for C₂₁H₂₄N₄O 475.0995, found 475.0971.

6-[(Dimethylamino)methyl]-3,4-dihydroisoquinolin-2(1H)-yl}(5-ethynyl-1-methyl-1H-pyrrolo[2,3-c]pyridin-2-yl)methanone (9f). NaOH (37 mg, 0.93 mmol) was added to a solution of ethyl 5-ethynyl-1-methyl-1H-pyrrolo[2,3-c]pyridine-2-carboxylate (60 mg, 0.26 mmol) in EtOH (absolute, 99.5%) (1.6 mL) and H₂O (0.160 mL). The mixture was stirred for 7 h at rt, followed by addition of acetic acid (0.2 mL) to neutralize an excess of NaOH. The solvent was evaporated followed by addition of H₂O and then the pH was adjusted to 2–3 by addition of HCl (aq, 1 M). The precipitated solid was filtered, washed with H₂O, and dried to provide 5-ethynyl-1-methyl-1H-pyrrolo[2,3-c]pyridine-2-carboxylic acid (34 mg, 65%). ¹H NMR (500 MHz, DMSO-*d*₆): δ 4.06 (s, 1H), 4.13 (s, 3H), 7.21 (s, 1H), 7.86 (s, 1H), 9.00 (s, 1H). MS (ESI) *m/z*: [M + H]⁺: 201.1.

General coupling method A was used with 5-ethynyl-1-methyl-1H-pyrrolo[2,3-c]pyridine-2-carboxylic acid (33 mg, 0.16 mmol). The residue was purified by preparative HPLC using basic conditions to provide **9f** (27 mg, 44%). ¹H NMR (600 MHz, DMSO-*d*₆): δ 2.15 (s, 6H), 2.86–2.96 (m, 2H), 3.35–3.38 (m, 2H), 3.69–3.97 (m, 5H), 4.06 (s, 1H), 4.86–4.70 (m, 2H), 6.75–6.85 (m, 1H), 6.98–7.27 (m, 3H), 7.83 (s, 1H), 8.94 (s, 1H). HRMS (ESI) *m/z*: [M + H]⁺ calcd for C₂₃H₂₅N₄O 373.2028, found 373.2040.

6-[(Dimethylamino)methyl]-3,4-dihydroisoquinolin-2(1H)-yl}[1-methyl-5-(trifluoromethyl)-1H-pyrrolo[2,3-c]pyridin-2-yl]methanone (9g). NaOH (53 mg, 1.33 mmol) was added to a solution of **8c** (102 mg, 0.37 mmol) in EtOH (absolute, 99.5%) (2.4 mL) and H₂O (0.4 mL). The mixture was stirred for 2.5 h at rt before addition of acetic acid (0.2 mL) to neutralize excess NaOH. The solvent was evaporated followed by addition of H₂O and then the pH was adjusted to 3 by addition of HCl (aq, 1 M). The precipitate was filtered, washed with H₂O, and dried to provide 1-methyl-5-(trifluoromethyl)-1H-pyrrolo[2,3-c]pyridine-2-carboxylic acid (71 mg, 78%). ¹H NMR (500 MHz, DMSO-*d*₆): δ 4.19 (s, 3H), 7.37 (s, 1H), 8.20 (s, 1H), 9.18 (s, 1H). MS (ESI) *m/z*: [M + H]⁺: 245.1.

General coupling method A was used with 1-methyl-5-(trifluoromethyl)-1H-pyrrolo[2,3-c]pyridine-2-carboxylic acid (35 mg, 0.14 mmol). The residue was purified by preparative HPLC using basic conditions to provide **9g** (46 mg, 76%). ¹H NMR (600 MHz, DMSO-*d*₆): δ 2.15 (s, 6H), 2.86–2.98 (m, 2H), 3.31–3.34 (m, 2H), 3.74 (s, 1H), 3.88–3.98 (m, 4H), 4.68–4.79 (m, 2H), 6.92–7.28 (m, 4H), 8.16 (d, *J* = 9.6 Hz, 1H), 9.11 (s, 1H). HRMS (ESI) *m/z*: [M + H]⁺ calcd for C₂₂H₂₄F₃N₄O 417.1902, found 417.1924.

6-[(Dimethylamino)methyl]-3,4-dihydroisoquinolin-2(1H)-yl}(1-methyl-5-phenyl-1H-pyrrolo[2,3-c]pyridin-2-yl)methanone (9h). General coupling method B was used with **8d** (42 mg, 0.15 mmol). The residue was purified by preparative HPLC using basic conditions to provide **9h** (14 mg, 22%). ¹H NMR (600 MHz, DMSO-*d*₆): δ 2.31–2.49 (m, 6H), 2.91–2.98 (m, 2H), 3.64–3.99 (m, 7H), 4.77–4.91 (m, 2H), 6.78–6.86 (m, 1H), 7.05–7.34 (m, 3H), 7.35–7.4 (m, 1H), 7.45–7.51 (m, 2H), 8.12 (dd, *J* = 1.2, 8.4 Hz, 2H), 8.15 (d, *J* = 8.0 Hz, 1H), 9.04 (s, 1H). HRMS (ESI) *m/z*: [M + H]⁺ calcd for C₂₇H₂₉N₄O 425.2341, found 425.2378.

2-[3-[(Dimethylamino)methyl]phenyl]propanenitrile (11). To a solution of **10** (2.0 g, 9.5 mmol) in 1,4-dioxane (100 mL) was added a solution of potassium [(dimethylamino)methyl]trifluoroborate (2.05 g, 12.4 mmol) in H₂O (20 mL), followed by addition of Pd(OAc)₂ (430 mg, 1.92 mmol), S-Phos (1.57 g, 3.83 mmol), and K₃PO₄ (16.23

g, 76.46 mmol). The resulting solution was stirred overnight at 100 °C under N₂. After cooling to rt, the solids were filtered out. The resulting mixture was concentrated under vacuum. The residue was applied onto a silica gel column eluting with chloroform:MeOH (100:1). This resulted in **11** (935 mg, 52%) as a colorless oil. ¹H NMR (400 MHz, CDCl₃): δ 1.65 (s, 3H), 2.24 (s, 6H), 3.27–3.64 (m, 2H), 3.89 (q, *J* = 7.3 Hz, 1H), 7.15–7.46 (m, 4H). MS (ESI) *m/z*: [M + H]⁺: 189. HPLC: *t*_R = 0.61 min.

2-[3-[(Dimethylamino)methyl]phenyl]propan-1-amine (12). To a solution of **11** (800 mg, 4.25 mmol) in MeOH (60 mL), was added Raney-Ni (1.0 g). The resulting reaction mixture was hydrogenated overnight at 25 °C under 20 psi of hydrogen pressure. After the completion of the reaction, the solids were filtered out. The resulting mixture was concentrated under vacuum. This resulted in **12** (770 mg, 94%) as a yellow oil, which was used directly in the next step without further purification. ¹H NMR (400 MHz, CDCl₃): δ 1.26 (d, *J* = 6.9 Hz, 3H), 2.25 (s, 6H), 2.75 (h, *J* = 6.8 Hz, 1H), 3.42 (d, *J* = 2.8 Hz, 2H), 7.07–7.19 (m, 3H), 7.20–7.30 (m, 2H). MS (ESI) *m/z*: [M + H]⁺: 193. HPLC: *t*_R = 0.86 min.

***N*-(2-[3-[(Dimethylamino)methyl]phenyl]propyl)formamide (13).** Into a 100 mL round-bottom flask was placed a solution of **12** (400 mg, 2.08 mmol) in methyl formate (20 mL). The resulting solution was stirred for 4.5 h at rt. The resulting mixture was concentrated under vacuum. The residue was purified by preparative TLC to yield **13** (396 mg, 86%) as a yellow oil. ¹H NMR (500 MHz, CDCl₃): δ 1.30 (d, *J* = 7.0 Hz, 3H), 2.25 (s, 6H), 2.97 (m, 1H), 3.29 (ddd, *J* = 4.9, 9.0, 13.7 Hz, 1H), 3.42 (d, *J* = 2.9 Hz, 2H), 3.72 (dt, *J* = 6.8, 13.5 Hz, 1H), 7.1–7.2 (m, 3H), 7.27–7.33 (m, 1H), 8.10 (s, 1H). MS (ESI) *m/z*: [M + H]⁺: 221. HPLC: *t*_R = 1.01 min.

***N*-(2-(3-Bromophenyl)ethyl)acetamide (15).**⁴⁶ To a stirred solution of **14** (2.0 g, 10 mmol) in DCM (10 mL) was added pyridine (10 mL) followed by slow addition of acetic chloride (799 mg, 10.2 mmol). The resulting solution was stirred for 2 h at 25 °C. The solids were filtered out. The resulting mixture was concentrated under vacuum. This resulted in **15** (2.0 g, 83%) as brown oil, which was used directly in the next step without further purification. MS (ESI) *m/z*: [M + H]⁺: 242. HPLC: *t*_R = 1.36 min.

6-Bromo-1-methyl-3,4-dihydroisoquinoline (16).⁴⁶ Oxalyl chloride (30.0 g, 238 mmol) was added to a stirred solution of **15** (5.00 g, 20.7 mmol) in DCM (50 mL) at 0 °C. The reaction mixture was then warmed to rt and stirred for 2 h. The mixture was cooled to –78 °C. FeCl₃ (20.0 g, 123 mmol) was added in. The resulting solution was warmed to 25 °C and stirred overnight. The solids were filtered out. The resulting mixture was concentrated under vacuum. The residue was dissolved in H₂SO₄:MeOH (1:10, 20 mL). The resulting solution was heated to 80 °C and stirred overnight. The resulting mixture was concentrated under vacuum and diluted with H₂O (100 mL). The pH was adjusted to 7 with ammonia (30%). The solids were filtered out. The resulting solution was extracted with DCM (3 × 200 mL). The organic layers were combined and concentrated under vacuum. This resulted in **16** (4.0 g, 86%) as yellow oil. ¹H NMR (400 MHz, DMSO-*d*₆, 26 °C): δ 2.28 (s, 3H), 2.65 (t, *J* = 7.6 Hz, 2H), 3.49–3.56 (m, 2H), 7.54–7.47 (m, 3H); MS (ESI) *m/z*: [M + H]⁺: 224. HPLC: *t*_R = 1.29 min.

Dimethyl[(4-methyl-3,4-dihydroisoquinolin-6-yl)methyl]amine (17a). Oxalyl chloride (6.21 g, 49 mmol) was added dropwise to a stirred solution of **13** (1.09 g, 4.95 mmol) in DCM (300 mL) at 0 °C. The reaction mixture was then warmed to rt and stirred for 2 h. Then the mixture was cooled to –78 °C. FeCl₃ (4.0 g, 25 mmol) was added. The resulting solution was warmed to 25 °C and stirred overnight. The solids were filtered out. The resulting mixture was concentrated under vacuum. The residue was dissolved in H₂SO₄:MeOH (1:10, 20 mL). The resulting solution was heated to 80 °C and stirred overnight. The resulting mixture was concentrated under vacuum and diluted with H₂O (10 mL). The pH value of the solution was adjusted to 7 with ammonia (30%). The solids were filtered out. The resulting mixture was extracted with DCM (3 × 200 mL). The organic layers were combined and concentrated under vacuum. The residue was purified by preparative TLC, this resulted in **17a** (550 mg, 55%) as a yellow oil. MS (ESI): *m/z*: [M + H]⁺: 203. HPLC: *t*_R = 0.28 min.

Dimethyl[(1-methyl-3,4-dihydroisoquinolin-6-yl)methyl]amine (17b). To a solution of **16** (100 mg, 0.45 mmol) in 1,4-dioxane (15 mL) was added potassium [(dimethylamino)methyl]-trifluoroborane (96 mg, 0.58 mmol), Pd(OAc)₂ (20 mg, 0.09 mmol), S-Phos (73 mg, 0.18 mmol), and a solution of K₃PO₄ (757 mg, 3.57 mmol) in H₂O (3 mL). The resulting solution was stirred for 2 h at 100 °C under N₂. After cooling to rt, the solids were filtered out. The resulting solution was extracted with DCM (5 × 5 mL). The organic layers were combined and concentrated under vacuum. The crude product was purified by preparative TLC with DCM:MeOH (10:1) to yield **17b** (66 mg, 73%) as a brown oil. MS (ESI) *m/z* [M + H]⁺: 203. HPLC: *t_R* = 0.18 min.

tert-Butyl 6-(Methoxy(methyl)carbamoyl)-3,4-dihydroisoquinoline-2(1H)-carboxylate (22). Compound **21** (2.00 g, 7.21 mmol) was dissolved in DCM (40 mL), 1-chloro-*N,N,N*-trimethylprop-1-en-1-amine (1.15 mL, 8.65 mmol) was added in one portion, and the mixture stirred at rt for 2 h. *N,O*-Dimethylhydroxylamine hydrochloride (1.41 g, 14.4 mmol) and TEA (4.0 mL, 29 mmol) were added, and the reaction mixture was stirred at rt for 14 h. Then the mixture was evaporated to dryness, redissolved in EtOAc, and washed sequentially with sodium bicarbonate (sat., 50 mL), brine (50 mL), and H₂O (50 mL). The organic phase was dried using Na₂SO₄, filtered, and evaporated to dryness to give **22** (2.1 g, 91%). ¹H NMR (400 MHz, CDCl₃): δ 1.50 (s, 9H), 2.87 (t, *J* = 5.6 Hz, 2H), 3.36 (s, 3H), 3.57 (s, 3H), 3.66 (t, *J* = 5.3 Hz, 2H), 4.61 (s, 2H), 7.14 (d, *J* = 7.9 Hz, 1H), 7.44–7.56 (m, 2H).

tert-Butyl 6-Acetyl-3,4-dihydroisoquinoline-2(1H)-carboxylate (23). Compound **22** (466 mg, 1.45 mmol) was dissolved in THF (10 mL) and then CH₃MgCl in THF (0.58 mL, 1.75 mmol) was added dropwise over 15 min at rt followed by stirring under nitrogen for 1 h. The reaction was quenched by addition of H₂O followed by extraction with MTBE (3 × 50 mL). The organic product was dried using Na₂SO₄ and evaporated to dryness. A clear oil of **23** (400 mg, quantitative yield) remained. ¹H NMR (400 MHz, CDCl₃): δ 1.50 (s, 9H), 2.59 (s, 3H), 2.90 (t, *J* = 5.7 Hz, 2H), 3.67 (t, *J* = 5.6 Hz, 2H), 4.63 (s, 2H), 7.20 (d, *J* = 8.0 Hz, 1H), 7.69–7.82 (m, 2H).

1-(2-(5-Bromo-1-methyl-1H-pyrrolo[2,3-c]pyridine-2-carbonyl)-1,2,3,4-tetrahydroisoquinolin-6-yl)ethanone (24). The amine **23** (50 mg, 0.29 mmol) was deprotected by dissolving the amine salt in 10% TFA in DCM for 6 h at rt and then evaporated to dryness. The resulting amine and 5-bromo-1-methyl-1H-pyrrolo[2,3-c]pyridine-2-carboxylic acid (80 mg, 0.31 mmol) were suspended in EtOAc (1070 μL) and TEA (119 μL, 0.86 mmol). The solution was cooled to 0 °C and T3P (182 mg, 0.29 mmol) was added dropwise to the cooled suspension. The reaction was then heated to 60 °C overnight. Then H₂O was added, followed by extraction with EtOAc. The organic phase was washed with brine, H₂O, sat. bicarbonate, and HCl (0.1 M) then dried using MgSO₄. The organic layer was evaporated to dryness to yield **24** (280 mg, 85%), which was used as is in the next step. ¹H NMR (500 MHz, DMSO-*d*₆): δ (mixture of rotamers) 2.57 (s, 3H), 2.97 (s, 2H), 3.57–4.04 (m, 5H), 4.79 (s, 1H), 4.92 (s, 1H), 6.76 (d, *J* = 19.1 Hz, 1H), 7.45 (d, *J* = 6.6 Hz, 1H), 7.82 (d, *J* = 9.3 Hz, 3H), 8.78 (s, 1H). MS (ESI) *m/z* [M + H]⁺: 412.0.

(5-Bromo-1-methyl-1H-pyrrolo[2,3-c]pyridin-2-yl)[6-[(dimethylamino)methyl]-4-methyl-3,4-dihydroisoquinolin-2(1H)-yl]methanone (25a). To a solution of **17a** (200 mg, 0.99 mmol) in MeOH (20 mL) was added NaBH₄ (42 mg, 1.10 mmol, 1.10 equiv) at 0 °C. The resulting solution was stirred for 1 h at 0 °C. The resulting mixture was concentrated under vacuum. The resulting solution was diluted with H₂O (10 mL) and extracted with DCM (3 × 5 mL). The organic layers were combined and concentrated under vacuum to yield **20a** (190 mg, 94%) as a colorless oil, which was used directly in the next step without further purification.

To a stirred solution of 5-bromo-1-methyl-1H-pyrrolo[2,3-c]pyridine-2-carboxylic acid (99 mg, 0.39 mmol) in DMF (10 mL) was added EDC (169 mg, 0.88 mmol), HOBt (72 mg, 0.53 mmol), and TEA (178 mg, 1.76 mmol). After being stirred for 30 min, **20a** (72 mg, 0.35 mmol) was added. The resulting reaction mixture was stirred for 3 h at 25 °C and then concentrated under vacuum. The solution was diluted with DCM (10 mL) and washed with H₂O (3 × 3 mL).

The organic layers were combined and concentrated under vacuum. The residue was purified by preparative TLC with DCM:MeOH (10:1). This resulted in **25a** (38 mg, 24%) as a white solid. ¹H NMR (DMSO-*d*₆, 300 MHz): δ 1.29–1.13 (m, 3H), 2.13 (s, 6H), 3.15–2.98 (m, 1H), 3.55–3.40 (m, 1H), 3.97–3.72 (m, 5H), 4.97–4.72 (m, 2H), 6.73 (s, 1H), 7.30–6.95 (m, 3H), 7.83 (s, 1H), 8.77 (s, 1H). HRMS (ESI) (*m/z*): [M + H]⁺ calcd for C₂₂H₂₆BrN₄O 441.1290, found 441.1316.

25e, (+)-isomer: [α]₂₀^D +23 (*c* 1.0, ACN); column, Chiralcel OJ, 250 × 4.6; flow rate, 4 mL/min; wavelength, PDA 240 nm; *t_R* = 2.70 min.

25f, (–)-isomer: [α]₂₀^D –24 (*c* 1.0, ACN); column: Chiralcel OJ, 250 × 4.6; flow rate, 4 mL/min; wavelength, PDA 240 nm; *t_R* = 3.85 min.

(5-Bromo-1-methyl-1H-pyrrolo[2,3-c]pyridin-2-yl)[6-[(dimethylamino)methyl]-1-methyl-3,4-dihydroisoquinolin-2(1H)-yl]methanone (25b). NaBH₄ (18 mg, 0.50 mmol) was added in portions to a stirred solution of **17b** (90 mg, 0.44 mmol) in MeOH (15 mL) at 0 °C. The solution was stirred for 1 h at 0 °C. The reaction mixture was diluted with H₂O (5 mL) and concentrated under vacuum. The remaining solution was extracted with DCM (4 × 5 mL). The organic layers were combined and concentrated under vacuum. This resulted in **20b** (60 mg, 59%) as a yellow oil, which was used in the next step without further purification. MS (ESI) *m/z* [M + H]⁺: 205. HPLC: *t_R* = 1.61 min.

To a solution of 5-bromo-1-methyl-1H-pyrrolo[2,3-c]pyridine-2-carboxylic acid (180 mg, 0.71 mmol) in DMF (20 mL) were added EDC (226 mg, 1.18 mmol), HOBt (159 mg, 1.18 mmol), and TEA (298 mg, 2.95 mmol). The mixture was stirred for 30 min, and then **20b** (121 mg, 0.59 mmol) was added. The resulting solution was stirred overnight at 25 °C, concentrated under vacuum, and finally diluted with DCM (50 mL). The organic phase was washed with H₂O (3 × 10 mL). The organic layer was concentrated under vacuum. The crude product was purified by preparative TLC with DCM:MeOH (10:1) to yield [[2-[[5-bromo-1-methyl-1H-pyrrolo[2,3-c]pyridin-2-yl]carbonyl]-1-methyl-1,2,3,4-tetrahydroisoquinolin-6-yl]methyl]-dimethylamine (160 mg, 51%) as a white solid. ¹H NMR (300 MHz, CD₃OD, 26 °C): δ 1.61–1.63 (m, 3H), 2.24 (s, 6H), 2.78–3.10 (m, 2H), 3.45–3.88 (m, 7H), 4.65–4.80 (m, 0.2H), 5.00–5.10 (m, 0.2H), 5.69–5.80 (m, 0.5H), 6.73 (s, 1H), 6.90–7.28 (m, 3H), 7.82 (s, 1H), 8.64–8.68 (m, 1H); HRMS (ESI) (*m/z*): [M + H]⁺ calcd for C₂₂H₂₆BrN₄O 441.1290, found 441.1307.

(5-Bromo-1-methyl-1H-pyrrolo[2,3-c]pyridin-2-yl)[6-[(dimethylamino)methyl]-3-methyl-3,4-dihydroisoquinolin-2(1H)-yl]methanone (25c). Into a 250 mL three-necked round-bottom flask, purged and maintained with an inert atmosphere of nitrogen, was placed a solution of **18** (2.00 g, 11.3 mmol) in 1,4-dioxane:H₂O (4:1, 60 mL). Potassium ((dimethylamino)methyl)trifluoroborate (2.78 g, 16.8 mmol), Pd(OAc)₂ (504 mg, 2.24 mmol), S-Phos (1.84 g, 4.49 mmol), and Cs₂CO₃ (36.52 g, 112.1 mmol) were added in. The resulting solution was stirred under inert atmosphere for 3 h at 100 °C. After cooling to rt, the solids were filtered out. The resulting solution was extracted with EtOAc (3 × 50 mL), and the organic layers were combined and concentrated under vacuum. The residue was purified on a silica gel column with EtOAc:hexane (1:2). This resulted in **19** (650 mg, 29%) as a yellow solid. MS (ESI) *m/z* [M + H]⁺: 201. HPLC: *t_R* = 0.31 min.

To a stirred solution of **19** (600 mg, 3.00 mmol) in MeOH (8 mL) was added aq concd HCl (320 mg) and PtO₂ (90 mg, 0.40 mmol) under N₂ atmosphere. The resulting solution was hydrogenated for 5 h at rt under 20 psi hydrogen pressure. The solids were filtered out. The resulting mixture was concentrated under vacuum. This resulted in **20c** (500 mg, 82%) as a yellow solid, which was used in the next step without further purification. MS (ESI) *m/z* [M + H]⁺: 205. HPLC: *t_R* = 0.21 min.

To a stirred solution of **20c** (73 mg, 0.36 mmol) in DMF (15 mL) were added 5-bromo-1-methyl-1H-pyrrolo[2,3-c]pyridine-2-carboxylic acid (100 mg, 0.39 mmol), HATU (150 mg, 0.39 mmol), TEA (43.8 mg, 0.43 mmol). The resulting solution was stirred for 3 h at rt. The reaction mixture was diluted with EtOAc (15 mL) and washed with NaHCO₃ (sat. 2 × 15 mL) and brine (2 × 15 mL). The resulting

mixture was concentrated under vacuum. The crude product was purified by preparative HPLC to give **25c** (90 mg, 57%) as a white solid. ^1H NMR (DMSO- d_6 , 300 MHz): δ 1.05–1.15 (m, 3H), 2.15 (s, 6H), 2.61–2.75 (m, 1H), 3.13–3.16 (m, 1H), 3.32–3.45 (m, 2H), 3.81 (s, 3H), 4.36–4.57 (m, 2H), 4.90–5.28 (m, 1H), 6.74 (s, 1H), 7.04–7.24 (m, 3H), 7.82 (s, 1H), 8.77 (s, 1H); HRMS (ESI) (m/z): $[\text{M} + \text{H}]^+$ calcd for $\text{C}_{22}\text{H}_{26}\text{BrN}_4\text{O}$ 441.1290, found 441.1302.

(5-Bromo-1-methyl-1H-pyrrolo[2,3-*c*]pyridin-2-yl){6-[1-(dimethylamino)ethyl]-3,4-dihydroisoquinolin-2(1H)-yl}methanone (**25d**). Compound **24** (40 mg, 0.10 mmol) was dissolved in a 33% MeNH₂ in ethanol solution (6 mL), and then 4 Å molecular sieves (500 mg) were added. The reaction mixture was heated to 50 °C for 40 min. Then sodium borohydride (3.67 mg, 0.10 mmol) was added followed by stirring for 4 h. The mixture was then quenched with H₂O and thereafter extracted with EtOAc (3 × 20 mL) followed by washing with brine and H₂O. The organic layer was dried over MgSO₄ and then evaporated to dryness. Then the second alkylation was performed. (5-Bromo-1-methyl-1H-pyrrolo[2,3-*c*]pyridin-2-yl)(6-(1-(methylamino)ethyl)-3,4-dihydroisoquinolin-2(1H)-yl)methanone (6 mg, 0.01 mmol) was dissolved in DCM (3 mL) and then formaldehyde (1.0 mL, 12 mmol) was added to this mixture. Sodium triacetoxyhydroborate (12 mg, 0.06 mmol) was added in one portion, followed by stirring at rt for 20 min. The reaction mixture was extracted using DCM (50 mL), washed with brine and H₂O, and dried over MgSO₄ to yield **25d** (6 mg, 21%). ^1H NMR (500 MHz, DMSO- d_6): δ (mixture of rotamers) 1.24 (d, $J = 6.2$ Hz, 3H), 2.08 (s, 6H), 2.90 (d, $J = 21.7$ Hz, 2H), 3.21 (d, $J = 5.7$ Hz, 1H), 3.29 (s, 1H), 3.61–4.03 (m, 5H), 4.69 (s, 1H), 4.82 (s, 1H), 6.75 (d, $J = 16.5$ Hz, 1H), 7.14 (d, $J = 24.5$ Hz, 3H), 8.77 (s, 1H). HRMS (ESI) (m/z): $[\text{M} + \text{H}]^+$ calcd for $\text{C}_{22}\text{H}_{25}\text{BrN}_4\text{O}$ 441.1290, found 441.1308.

Functional Assay (Inositol-1-phosphate). Cryopreserved, human QRFP (peptide P518/GPR103) receptor cell line (PerkinElmer) or CHO cells overexpressing either mouse GPR103A or GPR103B receptor⁸ (in house) were thawed in stimulation buffer and preincubated with compound at 37 °C in a humidified incubator with 5% CO₂. The cells were treated with *h*QRFP43 (Phoenix Pharmaceuticals) at EC₈₀ in stimulation buffer and incubated at 37 °C. After 50 min, reagents from the IP-1 Tb HTRF kit (CisBio Bioassays) were added and the resulting signal ratio (665 nm/620 nm) was measured in Pherastar (BMG). Reported values for *h*GPR103 IP-1 IC₅₀ are the mean of $N = 2$ –52 determinations. Within each determination of *h*GPR103 IP-1 IC₅₀, between one and three replicates at each concentration were used. The confidence interval ratio (CIR) was calculated to 2.0. Reported values for *m*GPR103A and B IP-1 IC₅₀ are a single determination or the mean of $N = 5$ –7 determinations. Within each determination of IC₅₀, between two or three replicates at each concentration were used.

Radioligand Binding Assay (RLB). Membranes from HEK cells overexpressing the human GPR103 receptor were incubated in 96-well microplates with compound and 0.25 nM radioligand [¹²⁵I]-*h*QRFP43 (NEX408, PerkinElmer) in binding buffer (50 mM Tris, pH 7.4, 1 mM EDTA, and 0.1% BSA) at 30 °C. After 90 min incubation, the reaction was filtered through filter plates (Whatman GF/C, 7700–4301) under vacuum; the plates were dried, treated with scintillation liquid, and counted in Trilux Microbeta (Wallac). Reported values are the mean of $N = 2$ –5 determinations with one replicate at each concentration. The confidence interval ratio (CIR) was calculated to 1.7.

Animals and Housing. Twenty-three female C57Bl/6 mice were used in the studies. The mice were housed in groups of at most six in Macrolon 2L cages (Scanbur, Karlslunde, Denmark) containing aspen wood chip bedding and an enriched environment with free access to food and water. The animal room had a regulated temperature (18–22 °C), humidity (50%), and a 12:12 h light–dark cycle. The mice were allowed at least 1 week of acclimatization before study initiation. To induce obesity mice were assigned to a high caloric diet (D12492 diet, 60% kcal as fat; Research Diets) at the age of 10 weeks for a period of 21 weeks. The study was approved by the local Animal Research Ethics Board Committee (Gothenburg, Sweden).

Food Intake Measurement. Obese female mice were housed individually for 7 days prior to the start of the experiment for

acclimatization purposes. Food intake was monitored using an in-house-built automatic monitoring system (AstraZeneca, R&D Mölndal, Sweden) allowing continuous measurement of food intake in undisturbed animals housed in their home cage environment. The mice had free access to two food hoppers and water. A feeding bout was defined as continuously feeding for more than five seconds, a minimum food intake (bout weight) of 10 mg, and a relapse time of 10 s between the bouts. The food intake was binned into hours and cumulative food intake was calculated. All data were collected using Microsoft Excel, and analysis was performed using Excel and Spotfire (TIBCO, Spotfire3.1.1, TIBCO Software Inc.) software. After 4 days of basal food intake registration, the animals (body mass 50–65 g) were dosed by oral gavage (5 mL/kg) with compound ($N = 7$ –8) or 5% mannitol vehicle ($N = 8$), twice daily for 3 days (first dose at the beginning of the dark phase and the second dose 7 h later). Food intake registration was performed during the whole period of the experiment. Compound-treated and vehicle groups were compared using ANOVA followed by Dunnett's multiple comparisons test.

Peptide Conformational Analysis: NMR Data Collection. QRFP26_(20–26) was purchased from Peptide Protein Research Ltd. (Fareham, UK). The peptide was dissolved to 100 mM in DMSO- d_6 ; aliquots of this stock solution were used to prepare samples for data acquisition. Samples were prepared at a range of concentrations (0.05–10 mM) in solutions of D₂O or H₂O, containing up to 10% residual DMSO- d_6 at pH 4, with 1 mM DSS- d_6 as an internal reference. 1D- and 2D-NMR spectra for the measurement of chemical shifts, temperature coefficients, and coupling constants were acquired at 500, 600, or 800 MHz at a range of temperatures (10–35 °C) with ¹³C- and ¹⁵N-edited experiments being performed at natural abundance. NOE restraints and coupling constants (³J_{HH}) used for structure determination were recorded using a 10 mM 90% H₂O:10% DMSO- d_6 sample at 800 MHz and 10 °C. The NOESY mixing time was 700 ms. Residual dipolar couplings were obtained using strained gels prepared using 7% (w/v) polyacrylamide as described previously⁴⁷ and soaked in a solution of 5 mM QRFP26_(20–26) in 85% H₂O:10% D₂O:5% DMSO- d_6 pH 4, before insertion into a suitably prepared 5 mm NMR tube. Coupling constants (¹J_{CH}, ¹J_{NH}) were measured from [¹H, ¹³C]-HSQC and [¹H, ¹⁵N]-HSQC spectra recorded without broadband heteronuclear decoupling during acquisition.

Chemical Shifts and Coupling Constants. All ¹H, ¹⁵N, and ¹³C chemical shifts and pertinent coupling constants of QRFP26_(20–26) in aqueous solution at pH 4 were assigned and measured using standard 1D- and 2D-NMR experiments (See Supporting Information, Supplementary Tables S1–S3).

Additional Peptide Characterization. Chemical shifts were measured at several solute concentrations (0.05–10 mM QRFP26_(20–26)) and at different temperatures (10–35 °C). Since the differences in ¹H chemical shifts between these conditions are small (<0.1 ppm) and all temperature-induced perturbations occur linearly (Supporting Information, Supplementary Table S3), it was concluded that QRFP26_(20–26) did not extensively self-associate in aqueous solution and that its solution structure was insensitive to changes in temperature in the range used in the present study. The N-terminal amine (Gly20 N) pK_a value was measured to be 8.0 ± 0.1, indicating that the dominant state of this moiety under physiological conditions was protonated; therefore, the peptide (including the arginine guanidinium group) carried a +2 charge under physiological conditions. Moreover, conformation-dependent coupling constants compared at pH 4 and 10 indicated that the molecule adopted the same shape in both charge states of the amine. Samples for measurement of structural restraints were therefore prepared using a pH value of 4, which maintained the molecule in its physiological charge state while minimizing the amide hydrogen exchange rate, thereby making them more amenable to NOE cross-peak observation (Supporting Information, Supplementary Table S2 and Supplementary Figures S1 and S2).

Measurement of Structural Restraints. Distance-restraint information was extracted by measuring the absolute values of NOE cross-peak heights. All possible NOE cross-peaks were measured, including overlapping peaks and those that were found to be

unambiguously zero. Peaks that could not be measured due to NMR artifacts were excluded. Scalar couplings were measured from resonance multiplet patterns in a high-resolution (800 MHz) 1D ^1H NMR experiment. Residual dipolar couplings were calculated from the difference in observed H–C or H–N splitting between sets of [^1H , ^{13}C]-HSQC and [^1H , ^{15}N]-HSQC spectra recorded in the free solution and aligned phase. In total, 809 structural restraints were used to define the dynamic 3D-structure of QRFP26_(20–26) (Supporting Information, Supplementary Tables S4–S7), comprising nuclear Overhauser enhancements (NOEs), scalar couplings, and residual dipolar couplings.

Structure Calculations. The structure of QRFP26_(20–26) was determined on the basis of the data described above, using a previously described method.⁴⁰ Briefly, an initial 3D-structure for QRFP26_(20–26) was built with fixed bond lengths and angles (based on geometrical constraints rather than by minimizing a computational chemistry energy function) which when compared with the Cambridge Structural Database (CSD)⁴⁸ using Mogul⁴⁹ had Z-scores less than 3. A structural ensemble for QRFP26_(20–26) was constructed by keeping all bonds and angles fixed and rotating the 24 rotatable bonds (see Supporting Information, Supplementary Figure S3). The rotation of torsions were matched to a set of mean angles, librations, and modal probabilities for each bond (termed the dynamic model). The ensemble thereby produced was used to predict the experimental data, and the fitness function χ^2 was calculated from comparison of these predictions with the measured experimental data. The dynamic model was iteratively refined to improve agreement between the predicted and measured NMR data until no further improvement was achieved (see Supporting Information, Supplementary Tables S4–S7 for final χ^2 -scores for each restraint). Pro-chiral stereoassignments were determined during structure calculations. Quality of fit measures were comparable with previous implementations of this structure determination method.⁴⁰ The conformational parameters for the final structure are detailed in the Supporting Information (Supplementary Table S9).

An ensemble, comprising 250 individual conformational states, was generated which can be considered representative of the conformational space occupied by the QRFP26_(20–26) molecule in solution.

Modeling. A conformational search on compound **9c** was done using mixed torsional/low-mode sampling in MacroModel⁵⁰ with default settings. **9c** was chosen as a substitute for **25e** due to the fact that the correct stereochemistry of **25e** was not assigned. The energy window for saving structures was set to 42.0 kJ/mol, and 100 steps/rotatable bond were used. Minimization was done using the OPLS2005 force field in water solvent with the PRCG method convergence gradient with the threshold set to 0.05. The global minimum according to molecular mechanics was found at least 10 times. The obtained conformations were superpositioned on the pyrrolo[2,3-*c*]pyridine scaffold of the global minima, and a full distance rmsd matrix was calculated using rmsd.py from Schrödinger. The rmsd matrix was clustered using the hierarchical clustering in spotfire (TIBCO, Spotfire3.1.1, TIBCO Software Inc.). The lowest energy conformation representative from each cluster and additional small variations of the methylenedimethyl amine side chain in the lowest energy clusters were optimized using Gaussian,⁵¹ with B3LYP, 6-31**+.

The C-terminal Arg-Phe motif of QRFP26_(20–26) was kept from one of the eight idealized peptide structures derived from eight dominant conformational families. The optimized structure of **9c** from quantum mechanics with best conformational fit to QRFP26_(20–26) was overlaid using the rigid alignment tool in MOE⁵² with the C-terminal Arg25-Phe26 motif fixed providing the overlay displayed in Figure 6. This conformation was found to be 0.8 kcal/mol higher than the lowest energy conformation identified after optimization with quantum mechanics and was considered a reasonable conformation of compound **9c**.

■ ASSOCIATED CONTENT

■ Supporting Information

Tables of the NMR data and the complete dynamic structural parameters of QRFP26_(20–26), additional figures relating to structure determination, and a detailed description of pK_a calculation, as well as assay descriptions for DMPK, *h*ERG, Nav1.5, and IKs. This material is available free of charge via the Internet at <http://pubs.acs.org>.

■ AUTHOR INFORMATION

Corresponding Author

*E-mail: Anneli.Nordqvist@astrazeneca.com. Tel: +46 31 776 2772.

Notes

The authors declare no competing financial interest.

■ ACKNOWLEDGMENTS

The authors would like to thank the Separation Science Group at AstraZeneca Mölndal for help with compound purification and Global DMPK for support with DMPK and physicochemical profiling.

■ ABBREVIATIONS USED

BID, twice daily; confidence interval ratio, CIR; CHO, Chinese hamster ovarian; DIEA, ethyldiisopropylamine; DMPK, drug metabolism and pharmacokinetics; EC_{80} , 80% of maximal effective concentration; EDC, 3-(ethyliminomethyleneamino)-*N,N*-dimethylpropan-1-amine; EtOAc, ethyl acetate; EtOH, ethanol; FIA, automated food intake measurement; GPR103, pyroglutamylated RF amide peptide receptor 103; *h*, human; HATU, *O*-(7-azabenzotriazol-1-yl)-1,1,3,3-tetramethyluronium hexafluorophosphate; *h*IKs, human cardiac slowly activating delayed rectifier K^+ channel; *h*Nav1.5, human cardiac sodium channel 1.5; HOBt, 1-hydroxybenzotriazole; IP-1, inositol-1-phosphate; LLE, lipophilic ligand efficiency; $\log D_{7.4}$, logarithm of the distribution coefficient in octanol/water at pH 7.4; *m*, mouse; MDR, minimum discriminatory ratio; MeCN, acetonitrile; MeOH, methanol; MTBE, methyl *tert*-butyl ether; PBS, phosphate-buffered saline; POMC, Pro-opiomelanocortin; RLB, radioligand binding assay; SEM, standard error of the mean; T3P, 1-propanephosphonic anhydride; TBTU, 2-(1*H*-benzo[*d*][1,2,3]triazol-1-yl)-1,1,3,3-tetramethylisouronium tetrafluoroborate; TEA, triethylamine; THIQ, tetrahydroisoquinoline

■ REFERENCES

- (1) Finucane, M. M.; Stevens, G. A.; Cowan, M. J.; Danaei, G.; Lin, J. K.; Paciorek, C. J.; Singh, G. M.; Gutierrez, H. R.; Lu, Y.; Bahalim, A. N.; Farzadfar, F.; Riley, L. M.; Ezzati, M. National, regional, and global trends in body-mass index since 1980: Systematic analysis of health examination surveys and epidemiological studies with 960 country-years and 9.1 million participants. *Lancet* **2011**, *377*, 557–567.
- (2) Nguyen, D. M.; El-Serag, H. B. The epidemiology of obesity. *Gastroenterol. Clin. North Am.* **2010**, *39*, 1–7.
- (3) Lee, D. K.; Nguyen, T.; Lynch, K. R.; Cheng, R.; Vanti, W. B.; Arkhitko, O.; Lewis, T.; Evans, J. F.; George, S. R.; O'Dowd, B. F. Discovery and mapping of ten novel G protein-coupled receptor genes. *Gene* **2001**, *275*, 83–91.
- (4) Jiang, Y.; Luo, L.; Gustafson, E. L.; Yadav, D.; Laverty, M.; Murgolo, N.; Vassileva, G.; Zeng, M.; Laz, T. M.; Behan, J.; Qiu, P.; Wang, L.; Wang, S.; Bayne, M.; Greene, J.; Monsma, F., Jr; Zhang, F. L. Identification and characterization of a novel RF-amide peptide

ligand for orphan G-protein-coupled receptor SP9155. *J. Biol. Chem.* **2003**, *278*, 27652–27657.

(5) Fukusumi, S.; Yoshida, H.; Fujii, R.; Maruyama, M.; Komatsu, H.; Habata, Y.; Shintani, Y.; Hinuma, S.; Fujino, M. A new peptidic ligand and its receptor regulating adrenal function in rats. *J. Biol. Chem.* **2003**, *278*, 46387–46395.

(6) Bruzzone, F.; Lectez, B.; Tollemer, H.; Leprince, J.; Dujardin, C.; Rachidi, W.; Chatenet, D.; Baroncini, M.; Beauvillain, J.; Vallarino, M.; Vaudry, H.; Chartrel, N. Anatomical distribution and biochemical characterization of the novel RFamide peptide 26RFa in the human hypothalamus and spinal cord. *J. Neurochem.* **2006**, *99*, 616–627.

(7) Chartrel, N.; Dujardin, C.; Anouar, Y.; Leprince, J.; Decker, A.; Clerens, S.; Do-Rego, J.; Vandesande, F.; Llorens-Cortes, C.; Costentin, J.; Beauvillain, J.; Vaudry, H. Identification of 26RFa, a hypothalamic neuropeptide of the RFamide peptide family with orexigenic activity. *Proc. Natl. Acad. Sci. U. S. A.* **2003**, *100*, 15247–15252.

(8) Takayasu, S.; Sakurai, T.; Iwasaki, S.; Teranishi, H.; Yamanaka, A.; Williams, S. C.; Iguchi, H.; Kawasaki, Y. I.; Ikeda, Y.; Sakakibara, I.; Ohno, K.; Ioka, R. X.; Murakami, S.; Dohmae, N.; Xie, J.; Suda, T.; Motoike, T.; Ohuchi, T.; Yanagisawa, M.; Sakai, J. A neuropeptide ligand of the G protein-coupled receptor GPR103 regulates feeding, behavioral arousal, and blood pressure in mice. *Proc. Natl. Acad. Sci. U. S. A.* **2006**, *103*, 7438–7443.

(9) Chartrel, N.; Alonzeau, J.; Alexandre, D.; Jeandel, L.; Alvarez-Perez, R.; Leprince, J.; Boutin, J.; Vaudry, H.; Anouar, Y.; Llorens-Cortes, C. The RFamide neuropeptide 26RFa and its role in the control of neuroendocrine functions. *Front. Neuroendocrinol.* **2011**, *32*, 387–397.

(10) Kampe, J.; Wiedmer, P.; Pfluger, P. T.; Castaneda, T. R.; Burget, L.; Mondala, H.; Kerr, J.; Liaw, C.; Oldfield, B. J.; Tschoep, M. H.; Bagnol, D. Effect of central administration of QRFP(26) peptide on energy balance and characterization of a second QRFP receptor in rat. *Brain Res.* **2006**, *1119*, 133–149.

(11) Le Marec, O.; Neveu, C.; Lefranc, B.; Dubessy, C.; Boutin, J. A.; Do-Rego, J.; Costentin, J.; Tonon, M.; Tena-Sempere, M.; Vaudry, H.; Leprince, J. Structure–activity relationships of a series of analogues of the RFamide-related peptide 26RFa. *J. Med. Chem.* **2011**, *54*, 4806–4814.

(12) Neveu, C.; Lefranc, B.; Tasseau, O.; Do-Rego, J.; Bourmaud, A.; Chan, P.; Bauchat, P.; Le Marec, O.; Chuquet, J.; Guilhaudis, L.; Boutin, J. A.; Segalas-Milazzo, I.; Costentin, J.; Vaudry, H.; Baudy-Floc'h, M.; Vaudry, D.; Leprince, J. Rational design of a low molecular weight, stable, potent, and long-lasting GPR103 aza-beta3-pseudopeptide agonist. *J. Med. Chem.* **2012**, *55*, 7516–7524.

(13) Thuau, R.; Guilhaudis, L.; Segalas-Milazzo, I.; Chartrel, N.; Oulyadi, H.; Boivin, S.; Fournier, A.; Leprince, J.; Davoust, D.; Vaudry, H. Structural studies on 26RFa, a novel human RFamide-related peptide with orexigenic activity. *Peptides* **2005**, *26*, 779–789.

(14) Do-Rego, J.; Leprince, J.; Chartrel, N.; Vaudry, H.; Costentin, J. Behavioral effects of 26RFamide and related peptides. *Peptides* **2006**, *27*, 2715–2721.

(15) Galusca, B.; Jeandel, L.; Germain, N.; Alexandre, D.; Leprince, J.; Anouar, Y.; Estour, B.; Chartrel, N. Orexigenic neuropeptide 26RFa: New evidence for an adaptive profile of appetite regulation in anorexia nervosa. *J. Clin. Endocrinol. Metab.* **2012**, *97*, 2012–2018.

(16) Yamamoto, T.; Wada, T.; Miyazaki, R. Analgesic effects of intrathecally administered 26RFa, an intrinsic agonist for GPR103, on formalin test and carrageenan test in rats. *Neuroscience* **2008**, *157*, 214–222.

(17) Lectez, B.; Jeandel, L.; El-Yamani, F.; Arthaud, S.; Alexandre, D.; Mardargent, A.; Jegou, S.; Mounien, L.; Bizet, P.; Magoul, R.; Anouar, Y.; Chartrel, N. The orexigenic activity of the hypothalamic neuropeptide 26RFa is mediated by the neuropeptide Y and proopiomelanocortin neurons of the arcuate nucleus. *Endocrinology* **2009**, *150*, 2342–2350.

(18) Haga, Y.; Mizutani, S.; Sato, N. Preparation of indole-2-carboxamide derivatives as QRFP receptor (GPR103) antagonists. WO2010126164A1, 2010.

(19) Kishino, H.; Mizutani, S.; Sakuraba, S.; Sato, N. Preparation of aryl indole derivatives as human QRFP receptor (GPR103) antagonists. WO2010117085A1, 2010.

(20) Fujimura, T.; Kishino, H.; Mizutani, T.; Sakuraba, S.; Sasaki, T.; Sato, N. Preparation of (hetero)aryl-substituted indolecarboxamides as GPR103 antagonists. WO2010119984A1, 2010.

(21) Nordqvist, A.; Kristensson, L.; Johansson, K. E.; Isaksson da Silva, K.; Fex, T.; Tyrchan, C.; Svensson Henriksson, A.; Nilsson, K. New hits as antagonists of GPR103 identified by HTS. *ACS Med. Chem. Lett.* **2014**, *5*, 527–532.

(22) Towart, R.; Linders, J. T. M.; Hermans, A. N.; Rohrbacher, J.; van, d. L.; Henk, J.; Ercken, M.; Cik, M.; Roevens, P.; Teisman, A.; Gallacher, D. J. Blockade of the IKs potassium channel: An overlooked cardiovascular liability in drug safety screening? *J. Pharmacol. Toxicol. Methods* **2009**, *60*, 1–10.

(23) Harmer, A. R.; Valentin, J. P.; Pollard, C. E. On the relationship between block of the cardiac Na⁺ channel and drug-induced prolongation of the QRS complex. *Br. J. Pharmacol.* **2011**, *164*, 260–273.

(24) Ho, G.; Emerson, K. M.; Mathre, D. J.; Shuman, R. F.; Grabowski, E. J. J. Carbodiimide-mediated amide formation in a two-phase system. A high-yield and low-racemization procedure for peptide synthesis. *J. Org. Chem.* **1995**, *60*, 3569–3570.

(25) Klapars, A.; Buchwald, S. L. Copper-catalyzed halogen exchange in aryl halides: An aromatic Finkelstein reaction. *J. Am. Chem. Soc.* **2002**, *124*, 14844–14845.

(26) Dyke, H. J.; Ellwood, C.; Gancia, E.; Gazzard, L. J.; Goodacre, S. C.; Kintz, S. S.; Lyssikatos, J. P.; MacLeod, C.; Williams, K. Diazacarbazoles as checkpoint kinase 1 inhibitors and their preparation and use in the treatment of cancer. WO2009151598A1, 2009.

(27) Briere, J.; Dupas, G.; Queguiner, G.; Bourguignon, J. Synthesis of fused systems in the isoquinoline series: Oxazolo- and pyrrolo[3,2-c]isoquinolines. *Heterocycles* **2000**, *52*, 1371–1383.

(28) Zhang, C.; Wang, Z.; Chen, Q.; Zhang, C.; Gu, Y.; Xiao, J. Copper-mediated trifluoromethylation of heteroaromatic compounds by trifluoromethyl sulfonium salts. *Angew. Chem., Int. Ed. Engl.* **2011**, *50*, 1896–1900.

(29) Colacot, T. J.; Shea, H. A. Cp₂Fe(PR₂)₂PdCl₂ (R = i-Pr, t-Bu) complexes as air-stable catalysts for challenging Suzuki coupling reactions. *Org. Lett.* **2004**, *6*, 3731–3734.

(30) Knorr, R.; Trzeciak, A.; Bannwarth, W.; Gillessen, D. New coupling reagents in peptide chemistry. *Tetrahedron Lett.* **1989**, *30*, 1927–1930.

(31) Basha, A.; Lipton, M.; Weinreb, S. M. A mild, general method for conversion of esters to amides. *Tetrahedron Lett.* **1977**, 4171–4174.

(32) Schonherr, H.; Cernak, T. Profound methyl effects in drug discovery and a call for new C-H methylation reactions. *Angew. Chem., Int. Ed.* **2013**, *52*, 12256–12267.

(33) Raushel, J.; Sandrock, D. L.; Josyula, K. V.; Pakyz, D.; Molander, G. A. Reinvestigation of aminomethyltrifluoroborates and their application in Suzuki–Miyaura cross-coupling reactions. *J. Org. Chem.* **2011**, *76*, 2762–2769.

(34) Larsen, R. D.; Reamer, R. A.; Corley, E. G.; Davis, P.; Grabowski, E. J. J.; Reider, P. J.; Shinkai, I. A modified Bischler–Napieralski procedure for the synthesis of 3-aryl-3,4-dihydroisoquinolines. *J. Org. Chem.* **1991**, *56*, 6034–6038.

(35) Caroon, J. M.; Clark, R. D.; Kluge, A. F.; Lee, C. H.; Strosberg, A. M. Synthesis and antihypertensive activity of a series of spiro[1,3,4,6,7,11b-hexahydro-2H-benzo[a]quinolizine-2,5'-oxazolidin-2'-one]s. *J. Med. Chem.* **1983**, *26*, 1426–1433.

(36) Mentzel, M.; Hoffmann, H. M. R. N-Methoxy N-methyl amides (Weinreb amides) in modern organic synthesis. *J. Prakt. Chem./Chem.—Ztg.* **1997**, *339*, 517–524.

(37) Escher, R.; Bünning, P. Synthesis of N-(1-carboxy-5-aminopentyl)dipeptides as inhibitors of angiotensin converting enzyme. *Angew. Chem., Int. Ed. Engl.* **1986**, *25*, 277–278.

(38) Lipinski, C. A.; Lombardo, F.; Dominy, B. W.; Feeney, P. J. Experimental and computational approaches to estimate solubility and

permeability in drug discovery and development settings. *Adv. Drug Delivery Rev.* **1997**, *23*, 3–25.

(39) Leeson, P. D.; Springthorpe, B. The influence of drug-like concepts on decision-making in medicinal chemistry. *Nat. Rev. Drug Discovery* **2007**, *6*, 881–890.

(40) Blundell, C. D.; Packer, M. J.; Almond, A. Quantification of free ligand conformational preferences by NMR and their relationship to the bioactive conformation. *Bioorg. Med. Chem.* **2013**, *21*, 4976–4987.

(41) Pierry, C.; Couve-Bonnaire, S.; Guilhaudis, L.; Neveu, C.; Marotte, A.; Lefranc, B.; Cahard, D.; Segalas-Milazzo, I.; Leprince, J.; Pannecoucke, X. Fluorinated pseudopeptide analogues of the neuropeptide 26RFa: Synthesis, biological, and structural studies. *Chem-BioChem.* **2013**, *14*, 1620–1633.

(42) LaPlante, S. R.; Nar, H.; Lemke, C. T.; Jakalian, A.; Aubry, N.; Kawai, S. H. Ligand bioactive conformation plays a critical role in the design of drugs that target the Hepatitis C virus NS3 protease. *J. Med. Chem.* **2014**, *57*, 1777–1789.

(43) Fujioka, M.; Omori, N. Subtleties in GPCR drug discovery: A medicinal chemistry perspective. *Drug Discovery Today* **2012**, *17*, 1133–1138.

(44) Murugaiah, A. M. S.; Wu, X.; Wallinder, C.; Mahalingam, A. K.; Wan, Y.; Skoeld, C.; Botros, M.; Guimond, M.; Joshi, A.; Nyberg, F.; Gallo-Payet, N.; Hallberg, A.; Alterman, M. From the first selective non-peptide AT2 receptor agonist to structurally related antagonists. *J. Med. Chem.* **2012**, *55*, 2265–2278.

(45) Perlman, S.; Costa-Neto, C. M.; Miyakawa, A. A.; Schambye, H. T.; Hjorth, S. A.; Paiva, A. C. M.; Rivero, R. A.; Greenlee, W. J.; Schwartz, T. W. Dual agonistic and antagonistic property of nonpeptide angiotensin AT1 ligands: Susceptibility to receptor mutations. *Mol. Pharmacol.* **1997**, *51*, 301–311.

(46) Henrich, M.; Weil, T.; Mueller, S.; Kauss, V.; Erdmare, E.; Zemribo, R. Preparation of 6-halopyrazolo[1,5-*a*]pyridines as mGluR5 modulators for the treatment of acute and/or chronic neurological disorders. WO2009095253A1, 2009.

(47) Tycko, R.; Blanco, F. J.; Ishii, Y. Alignment of biopolymers in strained gels: A new way to create detectable dipole–dipole couplings in high-resolution biomolecular NMR. *J. Am. Chem. Soc.* **2000**, *122*, 9340–9341.

(48) Allen, F. H. The Cambridge Structural Database: A quarter of a million crystal structures and rising. *Acta Crystallogr., Sect. B: Struct. Sci.* **2002**, *B58*, 380–388.

(49) Bruno, I. J.; Cole, J. C.; Edgington, P. R.; Kessler, M.; Macrae, C. F.; McCabe, P.; Pearson, J.; Taylor, R. New software for searching the Cambridge Structural Database and visualizing crystal structures. *Acta Crystallogr., Sect. B: Struct. Sci.* **2002**, *B58*, 389–397.

(50) *MacroModel, version 9.9*; Schrödinger, LLC, New York, 2012.

(51) Frisch, M. J.; Trucks, G. W.; Schlegel, H. B.; Scuseria, G. E.; Robb, M. A.; Cheeseman, J. R.; Scalmani, G.; Barone, V.; Mennucci, B.; Petersson, G. A.; Nakatsuji, H.; Caricato, M.; Li, X.; Hratchian, H. P.; Izmaylov, A. F.; Bloino, J.; Zheng, G.; Sonnenberg, J. L.; Hada, M.; Ehara, M.; Toyota, K.; Fukuda, R.; Hasegawa, J.; Ishida, M.; Nakajima, T.; Honda, Y.; Kitao, O.; Nakai, H.; Vreven, T.; Montgomery, J. A., Jr.; Peralta, J. E.; Ogliaro, F.; Bearpark, M.; Heyd, J. J.; Brothers, E.; Kudin, K. N.; Staroverov, V. N.; Kobayashi, R.; Normand, J.; Raghavachari, K.; Rendell, A.; Burant, J. C.; Iyengar, S. S.; Tomasi, J.; Cossi, M.; Rega, N.; Millam, J. M.; Klene, M.; Knox, J. E.; Cross, J. B.; Bakken, V.; Adamo, C.; Jaramillo, J.; Gomperts, R.; Stratmann, R. E.; Yazyev, O.; Austin, A. J.; Cammi, R.; Pomelli, C.; Ochterski, J. W.; Martin, R. L.; Morokuma, K.; Zakrzewski, V. G.; Voth, G. A.; Salvador, P.; Dannenberg, J. J.; Dapprich, S.; Daniels, A. D.; Farkas, Ö.; Foresman, J. B.; Ortiz, J. V.; Cioslowski, J.; Fox, D. J. *Gaussian 09, Revision D.01*; Gaussian, Wallingford, CT, 2009.

(52) *Molecular Operating Environment (MOE), version 2012.10*; Chemical Computing Group Inc., Montreal, Canada, 2012.